

# LTE-V2X Mode 3 scheduling based on adaptive spatial reuse of radio resources

Daniel Sempere-García, Miguel Sepulcre\* and Javier Gozalvez.

UWICORE Laboratory, Universidad Miguel Hernández de Elche (UMH), Avda. de la Universidad s/n, 03202 Elche, Spain.

E-mail addresses: [dsempere@umh.es](mailto:dsempere@umh.es), [msepulcre@umh.es](mailto:msepulcre@umh.es), [jgozalvez@umh.es](mailto:jgozalvez@umh.es).

\* Corresponding author.

**Abstract**—LTE-V2X (also known as C-V2X or Cellular V2X) introduces direct or sidelink V2V (Vehicle to Vehicle) communications using the PC5 interface. LTE-V2X defines two modes (Mode 3 and Mode 4) for the management of radio resources. This study focuses on Mode 3 where the cellular network manages and allocates the radio resources for direct or sidelink V2V communications. Contrary to Mode 4, the 3GPP standards do not define any concrete scheduling scheme to allocate resources under Mode 3. In this context, this paper proposes a context-based scheduling scheme for LTE-V2X Mode 3 that exploits the geographical location of vehicles and dynamically configures its operation with the objective that all vehicles experience a similar level of interference when resources must be shared. The proposed scheduling scheme, referred to as DIRAC (aDaptive spatIal Reuse of rAdio resourCes), is validated analytically and its performance is evaluated through system level simulations. The evaluation shows that DIRAC outperforms existing LTE-V2X Mode 3 and Mode 4 scheduling schemes and ensures a more scalable and stable network operation as the channel load and congestion increases.

**Keywords**—LTE-V2X; Vehicle to Everything; Vehicle to Vehicle; sidelink communications; PC5 interface; Mode 3 scheduling

## 1. INTRODUCTION

The 3GPP (3rd Generation Partnership Project) specified in Release 14 (and evolved in Release 15) a standard for V2X (Vehicle to Everything) communications [1] based on the LTE radio interface. This standard is known as LTE-V2X, C-V2X or Cellular V2X. The standard defines the PC5 interface for V2X sidelink or direct communications, and introduces two different modes for the management of the radio resources of the PC5 interface: Mode 3 and Mode 4. Mode 4 is a distributed mode that vehicles can use to autonomously select their radio resources using a sensing-based Semi-Persistent Scheduling (SPS) scheme. Mode 4 can operate without cellular coverage but its communications performance can be affected by a non-optimal radio resource selection based only on local sensing [2]. Mode 3 is a centralized mode where the cellular network selects the radio resources that vehicles utilize for direct or sidelink V2V communications (i.e. without using the Uu interface). Mode 3 can improve the QoS and scalability since the cellular network has a complete knowledge of the network status and the demand for resources from different vehicles. Mode 3 can then improve the resource selection and reduce interference among vehicles.

Unlike for Mode 4, the 3GPP standard does not specify a concrete scheduling scheme for Mode 3. Several schemes have been proposed in the literature and most of them exploit the geographical location of the vehicles to assign radio resources. Existing proposals either group vehicles in clusters to allocate resources or define heuristic solutions for allocating resources that are generally scenario-dependent. V2X networks are characterized by highly mobile conditions with constant changes in the network topology. This challenges the formation and management of clusters, and requires solutions that can dynamically adapt to the operating conditions and to changes in the scenario. To this aim, we present a novel context-based scheduling scheme for LTE-V2X Mode 3, DIRAC (aDaptive spatIal Reuse of rAdio resourCes), that adapts its operation to the scenario and context conditions. DIRAC exploits the geographical location of vehicles and dynamically configures its operation with the objective to ensure that all vehicles that must share radio resources with other vehicles experience similar interference levels. We compare the performance of DIRAC with a state-of-the-art LTE-V2X Mode 3 scheduling scheme and with the standardized sensing-based SPS Mode 4 scheduling scheme. The comparison shows that DIRAC increases the quality of V2V communications and the scalability of the V2X network. This is done through a better distribution of the impact of the interference and the consequent reduction of the probability of packet collisions. The proposal is validated against an analytical model that is also presented in this paper.

The paper is organized as follows. Section 2 reviews the state of the art and positions our proposed scheduling scheme. LTE-V2X Mode 3 is introduced in Section 3 and Section 4 presents DIRAC, our scheduling scheme. Section 5 presents the analytical performance model for DIRAC. Section 6 validates DIRAC and compares its performance and operation with a benchmark Mode 3 scheduling scheme as well as with the standardized sensing-based SPS Mode 4 scheduling scheme. Finally, Section 7 summarizes the conclusions of this study.

## 2. STATE OF THE ART

A significant number of studies have analyzed the performance of LTE-V2X Mode 4 and have proposed ways to improve the operation of its sensing-based semi-persistent scheduling scheme. For example, [3][4][5] optimize the parameters of the sensing-based SPS algorithm while [2][6] modify the sensing-based SPS algorithm and [7][8] propose alternative algorithms for vehicles to autonomously select the radio resources or sub-channels. On the other hand, there is only

a limited number of proposals of LTE-V2X Mode 3 scheduling algorithms. The majority of these proposals exploit the geographical location of the vehicles to assign radio resources. It should be noted that 3GPP standards already define procedures for vehicles to report their location to the cellular network [1][9]. The scheduling algorithms proposed for LTE-V2X Mode 3 can be classified in two categories. The first category includes proposals that exploit the proximity of nearby vehicles and organize vehicles into clusters. The second category of proposals consider vehicles individually and use the distance between vehicles to allocate radio resources using different heuristic algorithms. Within each of these two categories, proposals differ on their target when allocating radio resources. This is explained next in detail for each of the most relevant proposals per Mode 3 category.

The most relevant proposals in the category of cluster-based LTE-V2X Mode 3 studies include the proposals in [10], [11], [12] and [13]. The proposal in [10] clusters vehicles and defines the centralized resource allocation problem as a weighted bipartite graph matching that considers two disjoint sets: vehicles and sub-channels (represented as vertices of the graph). The connection between two vertices (a particular vehicle with a specific sub-channel) is called edge, and each edge has a weight that represents the bandwidth that a vehicle can achieve in that sub-channel. The goal of the algorithm is to find a perfect one-to-one vertex assignment that maximizes the system capacity defined in terms of achieved data rate. Each vehicle is assigned just one sub-channel and the proposal is designed to maintain a controlled computational complexity. To do so, authors propose two sub-optimal approaches with reduced complexity compared to an exhaustive search. Both proposals organize vehicles into overlapping clusters based on their location where only one vehicle in each cluster can transmit at a given time to avoid conflicts and packet collisions. The proposals offer interesting trade-offs between performance and complexity, but authors admit in [10] that, in practice, it is difficult to guarantee their assumption of having perfectly defined clusters. In fact, these clusters should be redefined as soon as vehicles change their location, so the resulting overhead can be significant. Further extensions were presented by the authors in [11] and [12] but again with the same clustering assumptions. The authors identify in [11] and [12] four allocation conditions in order to get conflict-free allocations. Moreover, they propose a mathematical framework to perform the allocations following these conditions, and two derived and simplified allocation schemes which can attain acceptable performance with lower complexity. However, as both studies are based on the same assumptions in [10], the same problems are observed in realistic mobility conditions. The cluster-based proposal in [13] solves some of the challenges related to the practical implementation of cluster-based schemes. To do so, the cellular network collects the location, speed and driving direction of the vehicles to predict their future locations and classify them in clusters. This information is used by the centralized scheduler to create more stable clusters and semi-persistently allocate the radio resources to all vehicles. Their goal is to reduce the number of collisions and the effect of In-Band Emissions (IBE) in order to ensure a high reliability in the

communications. This approach makes clusters more stable but also increases the complexity, and the complexity increases with the traffic density.

The rest of Mode 3 proposals belong to the second category where vehicles are considered individually and the resource allocation schemes utilize the location of vehicles to allocate resources. It is worth noting that our proposal is included in this category. The study in [14] introduces an analytical framework for location-based centralized scheduling. The framework explores the relation between the cell throughput, reliability and communication range. Using this framework, the authors demonstrate that there is an optimal scheduling distance between transmitting vehicles using the same resources (i.e. reuse distance) that maximizes the throughput while guaranteeing range and reliability restrictions; this is also the purpose of this study. The optimal distance is analytically derived based on requirements such as the communication range and outage probability. The outage probability is computed for a one-dimension highway scenario considering only the two nearest interferers. The study in [14] does not propose a particular centralized resource allocation algorithm but demonstrates analytically the existence and procedure to obtain the defined optimum distance; this is also validated by the authors using Monte Carlo simulations. It should be noted that the derived optimal distance depends on the scenario, propagation conditions and the specific application requirements. [15] presents a Mode 3 resource allocation solution that outperforms LTE-V2X Mode 4. The solution defines the resource allocation process as an optimization problem that seeks maximizing the packet reception ratio and hence increase the number of vehicles that receive a broadcasted packet broadcasted. The proposal uses the location of the vehicles to minimize the interference between vehicles using the same resources. However, [15] does not provide sufficient information about the algorithm (and hence cannot be replicated), and finding a globally optimal solution to the optimization problem can be computationally prohibitive as the traffic density increases. [16] presents another heuristic proposal in this category. The proposal is based on the concept of reuse range and awareness range. The reuse range is defined as the distance between transmitting vehicles using the same radio resource. The awareness range is defined as the distance at which transmitted packets should be received based on the application requirements. The reuse range was originally proposed in [17] and calculated in [16]. It is defined as the minimum distance between two vehicles sharing resources that guarantees the absence of interference at distances below the awareness range. Authors propose an algorithm that uses the location of the vehicles, the awareness range and the reuse range to allocate the resources so that the network capacity is maximized and the QoS requirements are guaranteed. The algorithm identifies radio resources that are not utilized by other vehicles at distances lower than the awareness and reuse ranges. In particular, the algorithm discards all the resources from the sub-frames that are used by any vehicle within the awareness range to avoid challenges resulting from the HD (half-duplex) nature of the radio transmissions; in HD, vehicles cannot receive packets while transmitting. In addition, the algorithm discards

those resources that are used by vehicles outside the awareness range but within the reuse range. This reduces the impact of interference but risks blocking transmissions if all radio resources are used by vehicles at distances lower than the reuse and awareness ranges. The algorithm then assigns randomly one of the remaining resources to each vehicle. Radio resources are assigned semi-persistently and new resources must be allocated to a vehicle as soon as a packet is received in error which can happen frequently in highly mobile environments. It should also be noted that the awareness range is application dependent, and it is not clear how it should be set in multi-application scenarios where the context of each vehicle (e.g. their speed) and application requirements vary. Finally, the same authors propose in [18] another location-based scheduling scheme that seeks to maximize the distance between vehicles using the same resources in order to control interference. Trying to maximize this distance can be a challenging task when the traffic density increases. In particular, it can lead to uneven allocations in which some vehicles that share a resource are separated by large distances while others are separated by short distances. This is visible in Fig. 1 that shows a simple example where we try maximizing the distance between vehicles that share resources. The example considers that there are four resources and that the distance between consecutive vehicles is  $D$ . Let us consider that vehicles request one resource at a time based on their index position: at  $t=1$ , vehicle 1 requests a resource, vehicle 2 requests a different resource at  $t=2$  and so on. The example considers four resources in the pool. In this case, vehicles 1 to 4 can be allocated initially different resources and avoid interference. This is not the case for vehicles 5 to 8 that have to reuse resources. If we want to maximize the distance between vehicles reusing resources, vehicle 5 is assigned the same resource as vehicle 1 and vehicle 6 is assigned the same resource as vehicle 4. However, vehicle 7 must share the same resource as vehicle 3 that is close. At  $t=8$ , the distances between vehicles using the same resource are:  $d(1,5)=6 \cdot D$ ,  $d(2,8)=4 \cdot D$ ,  $d(3,7)=2 \cdot D$  and  $d(4,6)=4 \cdot D$ . The distance between vehicles 1 and 5 that share a resource is three times the distance between vehicles 3 and 7 that also share a resource. This example shows that allocating resources with the intention to maximize the reuse distances can lead to uneven reuse distances that can degrade the QoS of certain vehicles.

Existing LTE-V2X Mode 3 scheduling schemes exhibit two major limitations. First, highly dynamic mobile environments significantly limit the stability and management of clusters. Second, many solutions require the selection of parameters for each particular scenario. Changes in the scenario require then a redesign of the solution, which limits their flexibility and applicability. To overcome these limitations, this paper presents a novel LTE-V2X Mode 3 scheduling scheme, DIRAC, which utilizes the location of the vehicles and the scenario and context conditions (e.g. the traffic density and channel load) to allocate resources to vehicles. DIRAC uses this information to allocate resources so that all vehicles in the scenario experience similar interference levels whenever resources must be shared as the load increases. The objective is to provide similar radio QoS performance to all vehicles and improve overall the reliability of sidelink V2X communications. To this aim, DIRAC computes first what should be the target distance between vehicles that

share radio resources to ensure that all pairs of interfering vehicles (i.e. vehicles sharing the resources) experience similar interference and QoS levels. DIRAC then allocates resources so that vehicles sharing resources (if there are none free) are at a distance as close as possible to the target distance. DIRAC adapts the target distance to the context conditions, e.g. to the traffic density, pool size or resources demanded by the vehicles.

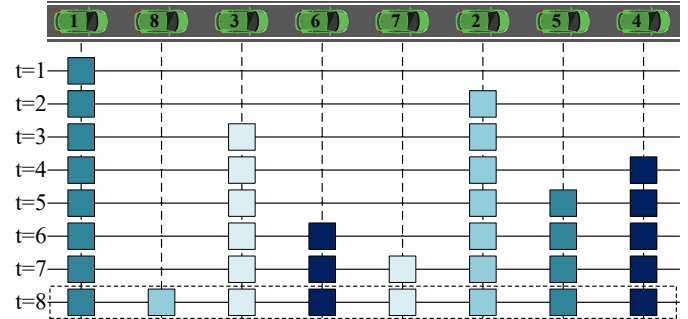


Fig. 1. Example of an allocation that tries maximizing the reuse distances.

### 3. LTE-V2X MODE 3

#### 3.1. Physical layer

LTE-V2X supports 10 and 20 MHz channel bandwidths. Each channel is organized in 1 ms sub-frames and sub-channels that correspond to a group of Resource Blocks (RBs) in the same sub-frame. An RB is 180 kHz wide in frequency (12 sub-carriers of 15 kHz) and the number of RBs per sub-channel can vary. LTE-V2X transmits data in Transport Blocks (TBs) over the Physical Sidelink Shared Channel (PSSCH). Control information is transmitted in Sidelink Control Information (SCI) messages over the Physical Sidelink Control Channel (PSCCH); an SCI occupies 2 RBs [19]. A data packet is transmitted in a TB together with its associated SCI in the same sub-frame. The SCI contains relevant information such as the Modulation and Coding Scheme (MCS) utilized to transmit the TB and the RBs occupied by the TB. This information must be correctly received by other vehicles to be able to decode the associated TB. A TB can occupy several sub-channels. The SCI is transmitted in the first two RBs of the first selected sub-channel while the TB occupies the following RBs in the same sub-frame [2]. SCIs are transmitted using QPSK modulation while TBs can be transmitted using QPSK, 16-QAM or 64-QAM modulations. LTE-V2X utilizes turbo coding and normal cyclic prefix. Each sub-carrier contains 14 symbols per sub-frame, four of which are set aside for Demodulation Reference Signals (DMRS) [1][20]. The maximum transmit power is 23 dBm and the sensitivity power level required at the receiver is -90.4 dBm [21].

#### 3.2. Mode 3 resource management

3GPP does not define a particular resource allocation or scheduling algorithm for LTE-V2X Mode 3. However, it defines the procedures needed to implement a centralized scheduling scheme. The vehicle or UE (User Equipment) needs to be in RRC\_CONNECTED mode to use Mode 3 transmissions. In this mode, all the parameters needed for the communication between the UE and the network are known by both entities, and a connection between the network and the UE has been established [1]. The UE must transmit a *SidelinkUEInformation* message to the eNB (Evolved Node B) to inform the network

that it is interested (or no longer interested) in receiving V2X sidelink messages. The same message is used to request or release dedicated resources for V2X sidelink communications. This message is sent from the UE to the eNB over the UL-DCCH (Uplink Dedicated Control Channel) logical channel. The UE may initiate the previously described requesting procedure upon successful connection establishment (when RRC\_CONNECTED mode is established in the UE) and upon acquisition of *SystemInformationBlockType21* (SIB21) or *SystemInformationBlockType26* (SIB26) from the eNB. The SIB21 and SIB26 IEs (Information Elements) contain configuration information for V2X sidelink communications and are included within the *SystemInformation* message. This message is broadcasted by the eNB over the BCCH (Broadcast Control Channel) or BR-BCCH (Bandwidth Reduced BCCH) logical channels [9].

Upon receiving the request for resources, the eNB schedules resources for transmitting the corresponding SCI and TB. Mode 3 supports dynamic and semi-persistent (SPS) scheduling. With dynamic scheduling, UEs ask for resources or sub-channels for transmitting each TB. This can increase the signaling overhead under high traffic densities and/or high packet transmission rates. With semi-persistent scheduling, the radio resources or sub-channels are assigned to each UE for a period of time. This period can be adapted to the transmission patterns [2][9].

A UE can report its location to the eNB and the eNB can use this information to schedule the resources. The UE can be configured to report its location via the existing *MeasurementReport* message over the UL-DCCH channel. This measurement reporting can be periodic or event-triggered. This study uses the existing functionality for vehicles to be able to periodically report their location to the eNB. The network configures the measurement reports using the *RRCConnectionReconfiguration* or *RRCConnectionResume* messages. In particular, the network can specify the reporting type (periodic or event-triggered) and configure the interval between periodical reports [9]. The *LocationInfo* IE within *measResults* is used to transfer location information available at the UE. The details of the procedures and messages described in this section can be found in [1][9].

#### 4. DIRAC SCHEDULING SCHEME

This section describes DIRAC, the LTE-V2X Mode 3 scheduling scheme proposed in this paper. The DIRAC scheduling scheme allocates the radio resources with the objective that all vehicles experience similar interference levels when they must share resources with other vehicles. DIRAC utilizes the location of the vehicles and the context conditions (e.g. the traffic density and channel load) to allocate resources. The DIRAC scheduling scheme computes first what should be the target distance between vehicles that share radio resources to ensure that all pairs of interfering vehicles (i.e. vehicles sharing the resources) experience similar interference and QoS levels. DIRAC allocates then resources so that vehicles sharing resources (if there are none free) are at a distance as close as possible to the target distance. DIRAC adapts the target distance to the context conditions. This minimizes the probability that two interfering vehicles are close to each other and therefore

these vehicles see their QoS degrade. To achieve its objectives, DIRAC exploits the geographical location of the vehicles and seeks to guarantee the same reuse and HD distances to all pairs of transmitting vehicles. The reuse distance is the distance between two transmitting vehicles that use the same resources. These two vehicles cannot detect each other and their transmissions interfere. The HD distance is the distance between two vehicles transmitting in the same sub-frame but in different sub-channels (or resources). LTE-V2X is half-duplex so vehicles cannot transmit and receive in the sub-frame. As a result, these two vehicles cannot detect each other but their transmissions do not interfere. To achieve a homogeneous distribution of interfering vehicles, DIRAC dynamically computes the target reuse and HD distances taking into account the context conditions, e.g. the traffic density. Table I lists the variables and parameters related to the design and operation the DIRAC algorithm.

TABLE I. VARIABLES UTILIZED IN THE PROPOSED DIRAC SCHEDULING SCHEME

Variable	Description
$d_{max}$	Total distance of all the roads in the cell covered by an eNB
$d_{reuse}$	Target reuse distance
$d_{HD}$	Target HD distance
$d(v_{req}, v_i)$	Distance between vehicles $v_{req}$ and $v_i$ (Step 3)
$N_{veh}$	Number of vehicles in the cell covered by an eNB
$N_{res}$	Number of resources in a pool
$N_{SF}$	Number of sub-frames
$N_{SC}$	Number of sub-channels
$N_{freeSF}$	Indicator of the number of completely free sub-frames (Step 1)
$N_{reuse}^{max}$	Maximum number of multiples of the $d_{reuse}$ (Step 3)
$N_{HD}^{max}$	Maximum number of multiples of the $d_{HD}$ (Step 3)
$v_{req}$	Vehicle requesting resources
$v_i$	Given vehicle in the scenario
$V(j,k)$	Set of vehicles using resource $(j,k)$ (Step 4)
$\lambda$	Packet transmission rate
$\Delta d_{reuse}(v_i)$	Difference between the distance $d(v_{req}, v_i)$ and $d_{reuse}$ (Step 3)
$\Delta d_{HD}(v_i)$	Difference between the distance $d(v_{req}, v_i)$ and $d_{HD}$ (Step 3)
$\Delta d_{reuse}^{(j,k)}$	Reuse metric for resource $(j,k)$ (Step 4)
$\Delta d_{HD}^{(j,k)}$	HD metric for resource $(j,k)$ (Step 4)
$\Delta d^{(j,k)}$	Metric for resource $(j,k)$ to select the allocated resource (Step 5)

##### 4.1. Target reuse and HD distances

DIRAC dynamically computes the target reuse and HD distances considering the number of vehicles in the cell covered by the serving eNB, the average distance between vehicles and the number of radio resources. All this information is available at the network with the current LTE-V2X standard. To compute the target distances, we define the number of vehicles in the cell as  $N_{veh}$ , and the total distance of all the roads in the cell covered by an eNB as  $d_{max}$ . The average distance between consecutive vehicles is  $d_{max}/N_{veh}$ . This average distance is computed assuming that vehicles are uniformly distributed in the cell. We denote as  $N_{res}$  the number of resources or sub-channels in a pool that the eNB manages. A pool is a set of sub-channels within a certain time period. This time period corresponds to a certain number of sub-frames, which is set according to the packet transmission interval.  $N_{res}$  can then be expressed as a function of the number of sub-frames ( $N_{SF}$ ) and the number of sub-channels ( $N_{SC}$ ). The number of sub-channels can be configured by the network and has been set to  $N_{SC}=2$  or 4 in this study. The number of sub-frames in the pool is calculated as 1000 divided by the

packet transmission rate ( $\lambda$ ), assuming 1 ms sub-frames. For example, if the packet transmission rate is  $\lambda=10$  pps, the pool will contain  $N_{SF}=1000/10=100$  sub-frames. If the number of sub-channels is  $N_{SC}=4$ , then the number of resources is  $N_{res}=400$ . Therefore,  $N_{res}$  can be calculated as follows:

$$N_{res} = N_{SF} \cdot N_{SC} = \frac{1000}{\lambda} \cdot N_{SC} \quad (1)$$

Without loss of generality, the following equation (2) defines the target reuse distance. DIRAC is designed so that vehicles allocated the same resource maintain a distance equal to the target reuse distance or one of its multiples. This distance is calculated as the number of resources ( $N_{res}$ ) multiplied by  $d_{max}/N_{veh}$ , where  $d_{max}/N_{veh}$  is the average distance between consecutive vehicles in the cell as defined previously. Since the pool has  $N_{res}$  resources, the multiplication of this distance by  $N_{res}$  is the minimum distance between two vehicles that share the same resource. We can illustrate this with the example shown in Fig. 2 and Fig. 3. In this example, we consider that the total number of resources in the pool is  $N_{res}=400$ . As a consequence, the first 400 vehicles in Fig. 2 could be allocated following the indexes of Fig. 3. If the number of vehicles was equal to 400, there would be no need that two vehicles reuse the same resource. However, if the number of vehicles is higher, resources will need to be shared. This allocation of the resources is done in order to ensure an equal target reuse distance (or one of its multiples) between any pair of vehicles sharing resources. Consequently, vehicle 1 is allocated the first resource of Fig. 3 and shares it with vehicle 401. Vehicle 2 shares its resource with vehicle 402, and so on. This implies that the distance between pairs of vehicles sharing a resource would be equal for all of them according to equation (2) (if they were uniformly distributed), or equal to a multiple of the target reuse distance. Vehicles 1, 401, 801, 1201 etc. would be allocated the first resource of Fig. 3. These vehicles would be located at a distance between them equal to the target reuse distance and its multiples.

$$d_{reuse} = N_{res} \cdot \frac{d_{max}}{N_{veh}} \quad (2)$$

On the other side, vehicles 1, 101, 201 and 301 in Fig. 3 experience the HD effect since they utilize resources in the same sub-frame. Extrapolating this to any sub-frame of the pool, the target HD distance  $d_{HD}$  between vehicles using resources on the sub-frame can be expressed as:

$$d_{HD} = N_{SF} \cdot \frac{d_{max}}{N_{veh}} \quad (3)$$

It is worth noting that the simple example in Fig. 2 and Fig. 3 is utilized with illustration purposes to derive the expressions of the target reuse and HD distances. When applying the DIRAC scheduling scheme in a realistic scenario (highway or urban), the target distances are calculated dynamically through (2) and (3) by the eNB upon the reception of a resource request from a vehicle. In this way, the eNB updates the distances according to the current context for every request. The resource allocation is only performed for the vehicle which makes the request, so the previously allocated vehicles maintain their assigned resources. It is also important to note that DIRAC is not restricted to a uniform distribution of vehicles despite the assumptions made in equations (2) and (3). These equations are used as a reference

in the resource allocation process but DIRAC can be applied in any scenario. In fact, DIRAC is evaluated in this study in urban and highway scenarios where vehicles are not uniformly distributed.

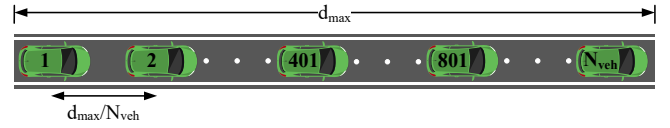


Fig. 2. Example scenario considered to calculate the target distances.

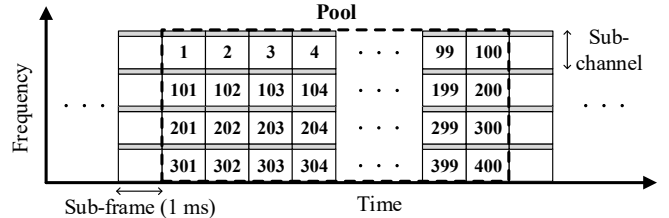


Fig. 3. Resource pool with  $N_{SF}=100$  sub-frames and  $N_{SC}=4$  sub-channels.

#### 4.2. Algorithm

The DIRAC scheduling scheme is executed by the eNB (central scheduler) every time it receives a request from a vehicle for radio resources for a V2X sidelink transmission. The process to allocate a resource (or sub-channel) has the following five steps (Fig. 4).

*Step 1.* The eNB searches if there is any completely free sub-frame, i.e. a sub-frame where none of its sub-channels have been allocated. If there are free sub-frames (line 1 of Algorithm I), the eNB randomly selects one of them and randomly assigns to the requesting vehicle one sub-channel of the selected sub-frame (lines 2-6 of Algorithm I). This sub-channel prevents packet collisions and the HD effect. It should be noted that free sub-frames exist if  $N_{veh} \leq N_{SF}$  and thus the channel load is low. In this case, steps (2)-(5) are not executed.

---

Algorithm I. Step 1. DIRAC scheduling scheme  
 Inputs:  $N_{SF}$ ,  $N_{SC}$ ,  $N_{veh}$ ,  $N_{freeSF}$ ,  $freeSubframes$  list  
 Output: selected resource  $(j,k)$  for requesting vehicle  $v_{req}$   
 Execution: every time a vehicle  $v_{req}$  requests resources and  $N_{freeSF} > 0$

---

1. **If**  $N_{freeSF} > 0$  **then**
  2.     Generate random number  $1 \leq i \leq N_{freeSF}$
  3.     Select sub-frame  $j$  equal to  $freeSubframes(i)$
  4.     Remove element  $freeSubframes(i)$
  5.      $N_{freeSF}$  equal to  $N_{freeSF} - 1$
  6.     Select random sub-channel  $0 \leq k \leq N_{SC}-1$  within sub-frame  $j$
  7. **End if**
- 

*Step 2.* If there is no free sub-frame, the DIRAC scheduling scheme looks for free sub-channels (i.e. sub-channels that have not been allocated yet to any vehicle) or for sub-channels that are assigned to vehicles at a distance close to the target reuse and HD distances (or one of their multiples). To this aim, the DIRAC scheduling scheme uses the location of vehicles that have already been assigned sub-channels. The eNB computes the target reuse ( $d_{reuse}$ , line 1 of Algorithm II) and HD ( $d_{HD}$ , line 2 of Algorithm II) distances following (2) and (3).

Algorithm II. *Step 2.* DIRAC scheduling scheme

Inputs:  $N_{SF}$ ,  $N_{SC}$ ,  $N_{veh}$ ,  $N_{freeSF}$ ,  $freeSubframes$  list

Output: computed target distances  $d_{reuse}$  and  $d_{HD}$

Execution: every time a vehicle  $v_{req}$  requests resources and  $N_{freeSF} = 0$

1. Compute  $d_{reuse}$  with equation (2)
2. Compute  $d_{HD}$  with equation (3)

*Step 3.* DIRAC calculates the distance between the vehicle requesting sub-channels ( $v_{req}$ ) and all the vehicles that have already been allocated sub-channels in the pool (line 2 of Algorithm III). The distance between  $v_{req}$  and a given vehicle  $v_i$  is referred to as  $d(v_{req}, v_i)$ .  $d(v_{req}, v_i)$  is then compared to the target reuse distance calculated in Step 2 (lines 7-12 of Algorithm III). It is possible that  $d(v_{req}, v_i)$  is not close to the reuse distance but to a multiple of the reuse distance. The comparison is then conducted using the following equation:

$$\Delta d_{reuse}(v_i) = \min_{n \in \mathbb{N}} (|d(v_{req}, v_i) - n \cdot d_{reuse}|) \quad (4)$$

In this equation,  $n$  is a positive integer number ( $1 \leq n \leq N_{reuse}^{max}$  with  $N_{reuse}^{max} = \lfloor d_{max}/d_{reuse} \rfloor$ ) that is used to compare  $d(v_{req}, v_i)$  with any integer multiple of  $d_{reuse}$ . If the difference computed in equation (4) is small,  $v_{req}$  and  $v_i$  are candidates to reuse the same sub-channel. This process is repeated to compare  $d(v_{req}, v_i)$  and the target HD distance ( $d_{HD}$ ) (and its multiples) as follows (lines 13-18 of Algorithm III):

$$\Delta d_{HD}(v_i) = \min_{n \in \mathbb{N}} (|d(v_{req}, v_i) - n \cdot d_{HD}|) \quad (5)$$

where  $n$  is also a positive integer number with  $1 \leq n \leq N_{HD}^{max}$  and  $N_{HD}^{max} = \lfloor d_{max}/d_{HD} \rfloor$ . If the difference computed in equation (5) is small,  $v_{req}$  and  $v_i$  are candidates to use a sub-channel in the same sub-frame.

Algorithm III. *Step 3.* DIRAC scheduling scheme

Inputs:  $N_{SF}$ ,  $N_{SC}$ ,  $N_{veh}$ ,  $N_{freeSF}$ ,  $freeSubframes$  list

Output: computed  $\Delta d_{reuse}(v_i)$  and  $\Delta d_{HD}(v_i)$  for every vehicle allocated in the pool

Execution: every time a vehicle  $v_{req}$  requests resources and  $N_{freeSF} = 0$

1. **For** each vehicle  $v_i$  in the scenario with  $1 \leq v_i \leq N_{veh} - 1$  **do**
2. Get the distance  $d(v_{req}, v_i)$  between  $v_{req}$  and  $v_i$
3. Set  $\Delta d_{reuse}(v_i)$  equal to 0
4. Set  $\Delta d_{HD}(v_i)$  equal to 0
5. Set  $N_{reuse}^{max}$  equal to  $\lfloor d_{max}/d_{reuse} \rfloor$
6. Set  $N_{HD}^{max}$  equal to  $\lfloor d_{max}/d_{HD} \rfloor$
7. **For** each  $n_1$  with  $1 \leq n_1 \leq N_{reuse}^{max}$  **do**
8. Compute  $aux_{reuse}$  equal to  $\text{abs}(d(v_{req}, v_i) - n_1 \cdot d_{reuse})$
9. **If**  $aux_{reuse} > \Delta d_{reuse}(v_i)$  **then**
10. Set  $\Delta d_{reuse}(v_i)$  equal to  $aux_{reuse}$
11. **End if**
12. **End for**
13. **For** each  $n_2$  with  $1 \leq n_2 \leq N_{HD}^{max}$  **do**
14. Compute  $aux_{HD}$  equal to  $\text{abs}(d(v_{req}, v_i) - n_2 \cdot d_{HD})$
15. **If**  $aux_{HD} > \Delta d_{HD}(v_i)$  **then**
16. Set  $\Delta d_{HD}(v_i)$  equal to  $aux_{HD}$
17. **End if**
18. **End for**
19. **End for**

*Step 4.* DIRAC then computes two metrics (one related to the reuse distances  $\Delta d_{reuse}^{(j,k)}$ , and another related to the HD distances  $\Delta d_{HD}^{(j,k)}$ ) for all the sub-channels to decide in Step 5 which one should be assigned to the vehicle requesting sub-channels. To this aim, we have to take into account that multiple

vehicles could be using a given sub-channel, and each of these vehicles could be at a different distance to the requesting vehicle  $v_{req}$  and hence have a different  $\Delta d_{reuse}(v_i)$  or  $\Delta d_{HD}(v_i)$ . Moreover, there could be free sub-channels that must be also considered, as explained later. In this case, DIRAC computes the reuse metric  $\Delta d_{reuse}^{(j,k)}$  for each occupied sub-channel of the pool ( $j, k$ ) where  $j$  is the sub-frame and  $k$  is the sub-channel. To do so, DIRAC computes the maximum  $\Delta d_{reuse}(v_i)$  for all vehicles  $v_i$  using a certain sub-channel (lines 9-11 of Algorithm IV). For sub-channel ( $j, k$ ), the reuse metric is expressed as:

$$\Delta d_{reuse}^{(j,k)} = \max_{v_i \in V(j,k)} (\Delta d_{reuse}(v_i)) \quad (6)$$

where  $V(j, k)$  is the set of vehicles using sub-frame  $j \in [0, N_{SF} - 1]$  and sub-channel  $k \in [0, N_{SC} - 1]$ . An analogous process is followed to calculate the HD metric  $\Delta d_{HD}^{(j,k)}$  for each occupied sub-channel ( $j, k$ ) although some changes are necessary (lines 12-14 and 21-33 of Algorithm IV). In this case, the metric  $\Delta d_{HD}^{(j,k)}$  for sub-channel ( $j, k$ ) is computed considering the differences of the distances between all vehicles that are using sub-frame  $j$  but are not using sub-channel  $k$ . This is the case because these vehicles will suffer from the HD effect if the requesting vehicle is allocated the sub-channel ( $j, k$ ). This is expressed as:

$$\Delta d_{HD}^{(j,k)} = \max_{v_i \in V(j, \bar{k})} (\Delta d_{HD}(v_i)) \quad (7)$$

where  $V(j, \bar{k})$  is the set of vehicles using sub-frame  $j \in [0, N_{SF} - 1]$  but not using sub-channel  $k \in [0, N_{SC} - 1]$ .

DIRAC must also consider the free sub-channels ( $j_f, k_f$ ) that are not used by any vehicle. To do so, DIRAC computes the reuse and HD metrics for the free sub-channels as the minimum metrics  $\Delta d_{reuse}^{(j,k)}$  and  $\Delta d_{HD}^{(j,k)}$  obtained through (6) and (7) for all the occupied resources, respectively (lines 18, 31 and 35-44 of Algorithm IV). This is done so that DIRAC assigns the free resources with high probability.

Algorithm IV. *Step 4*. DIRAC scheduling scheme

Inputs:  $N_{SF}$ ,  $N_{SC}$ ,  $N_{veh}$ ,  $N_{freeSF}$ ,  $freeSubframes$  list  
 Output: computed  $\Delta d_{reuse}^{(j,k)}$  and  $\Delta d_{HD}^{(j,k)}$  for every resource  $(j,k)$   
 Execution: every time a vehicle  $v_{req}$  requests resources and  $N_{freeSF} = 0$

```

1. Set  $\Delta d_{reuse}^{min}$  equal to  $Inf$ 
2. Set  $\Delta d_{HD}^{min}$  equal to  $Inf$ 
3. For each sub-frame  $j$  with  $0 \leq j \leq N_{SF}-1$  do
4.   For each sub-channel  $k$  with  $0 \leq k \leq N_{SC}-1$  do
5.     Set  $\Delta d_{reuse}^{(j,k)}$  equal to -1 for resource  $(j,k)$ 
6.     Set  $\Delta d_{maxHD}^{(j,k)}$  equal to -1 for resource  $(j,k)$ 
7.     For each vehicle  $v_i$  in the scenario with  $1 \leq v_i \leq N_{veh}-1$  do
8.       If  $v_i$  is using resource  $(j,k)$  then
9.         If  $\Delta d_{reuse}(v_i) > \Delta d_{reuse}^{(j,k)}$  then
10.          Set  $\Delta d_{reuse}^{(j,k)}$  equal to  $\Delta d_{reuse}(v_i)$ 
11.         End if
12.         If  $\Delta d_{HD}(v_i) > \Delta d_{maxHD}^{(j,k)}$  then
13.          Set  $\Delta d_{maxHD}^{(j,k)}$  equal to  $\Delta d_{HD}(v_i)$ 
14.         End if
15.       End if
16.     End for
17.   If  $\Delta d_{reuse}^{(j,k)} < \Delta d_{reuse}^{min}$  and  $\Delta d_{reuse}^{(j,k)} \neq -1$  then
18.     Set  $\Delta d_{reuse}^{min}$  equal to  $\Delta d_{reuse}^{(j,k)}$ 
19.   End if
20. End for
21. For each sub-channel  $k$  with  $0 \leq k \leq N_{SC}-1$  do
22.   Set  $\Delta d_{HD}^{(j,k)}$  equal to -1 for resource  $(j,k)$ 
23.   For each sub-channel  $k_2$  with  $0 \leq k_2 \leq N_{SC}-1$  do
24.     If  $k \neq k_2$  then
25.       If  $\Delta d_{maxHD}^{(j,k)} > \Delta d_{HD}^{(j,k)}$  then
26.         Set  $\Delta d_{HD}^{(j,k)}$  equal to  $\Delta d_{maxHD}^{(j,k)}$ 
27.       End if
28.     End if
29.   End for
30.   If  $\Delta d_{HD}^{(j,k)} < \Delta d_{HD}^{min}$  and  $\Delta d_{HD}^{(j,k)} \neq -1$  then
31.     Set  $\Delta d_{HD}^{min}$  equal to  $\Delta d_{HD}^{(j,k)}$ 
32.   End if
33. End for
34. End for
35. For each sub-frame  $j$  with  $0 \leq j \leq N_{SF}-1$  do
36.   For each sub-channel  $k$  with  $0 \leq k \leq N_{SC}-1$  do
37.     If  $\Delta d_{reuse}^{(j,k)}$  equal to -1 then
38.       Set  $\Delta d_{reuse}^{(j,k)}$  equal to  $\Delta d_{reuse}^{min}$ 
39.     End if
40.     If  $\Delta d_{HD}^{(j,k)}$  equal to -1 then
41.       Set  $\Delta d_{HD}^{(j,k)}$  equal to  $\Delta d_{HD}^{min}$ 
42.     End if
43.   End for
44. End for
    
```

*Step 5*. The eNB assigns to  $v_{req}$  the sub-channel with the smallest sum of its metrics:  $\Delta d^{(j,k)} = \Delta d_{reuse}^{(j,k)} + \Delta d_{HD}^{(j,k)}$ , i.e. the sub-channel that guarantees being closer to the target distances (Algorithm V).

Algorithm V. *Step 5*. DIRAC scheduling scheme

Inputs:  $N_{SF}$ ,  $N_{SC}$ ,  $N_{veh}$ ,  $N_{freeSF}$ ,  $freeSubframes$  list  
 Output: selected resource  $(j,k)$  for requesting vehicle  $v_{req}$   
 Execution: every time a vehicle  $v_{req}$  requests resources and  $N_{freeSF} = 0$

```

1. Set  $\Delta d_{min}$  equal to  $Inf$ 
2. For each sub-frame  $j$  with  $0 \leq j \leq N_{SF}-1$  do
3.   For each sub-channel  $k$  with  $0 \leq k \leq N_{SC}-1$  do
4.     Compute  $\Delta d^{(j,k)}$  equal to  $\Delta d_{reuse}^{(j,k)} + \Delta d_{HD}^{(j,k)}$ 
5.     If  $\Delta d^{(j,k)} < \Delta d_{min}$  then
6.       Set  $\Delta d_{min}$  equal to  $\Delta d^{(j,k)}$ 
7.       Select resource  $(j,k)$  as the best
8.     End if
9.   End for
10. End for
    
```

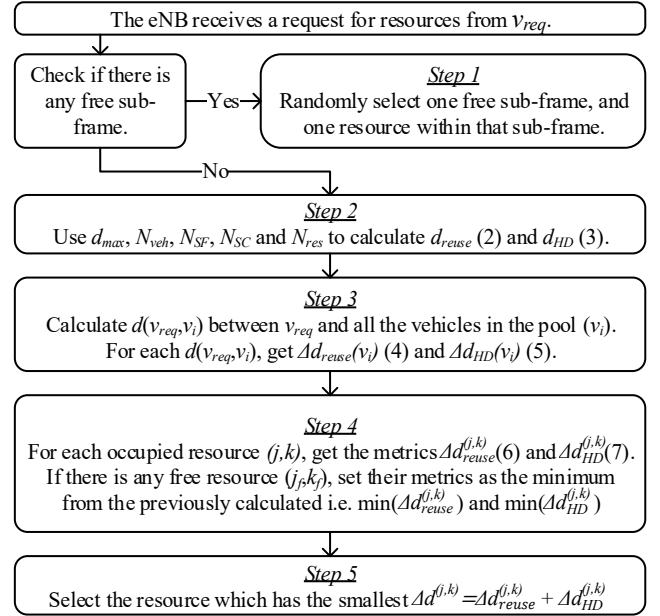


Fig. 4. Flow diagram for the DIRAC scheduling scheme.

Due to the vehicles' mobility, the resource assignment should not be maintained for a long period of time. To this aim, DIRAC assigns the allocated resources semi-persistently following the 3GPP standards. Following the 3GPP specifications for Mode 4, we set *Reselection Counter* as a random number between: 5 and 15 if the vehicle transmits 10 pps; 10 and 30 for 20 pps; and 25 and 75 for 50 pps. *Reselection Counter* is decremented by one after each packet transmission and the vehicle requests again resources once *Reselection Counter* is equal to zero. This results in that, on average, each vehicle requests new resources every second.

The DIRAC scheduling scheme has been illustrated in this section using a scenario with one driving direction. However, it is completely valid for more complex scenarios with multiple lanes and different driving directions as well as for highway, urban and suburban scenarios. This is the case because the central scheduler only needs to know the location of the vehicles to assign the resources.

## 5. ANALYTICAL MODEL

This section presents an analytical performance model of the DIRAC scheduling scheme. The model quantifies the PDR (Packet Delivery Ratio) that can be achieved with our proposed scheduling scheme, DIRAC, as a function of the distance between the transmitter and the receiver. This model is openly available in [22] so that other researchers can easily compare the performance of their scheduling scheme with the solution proposed in this paper. To model the PDR, the following four mutually exclusive errors present in LTE-V2X [23] are quantified:

- 1) Errors due to half-duplex transmissions (*HD*). The LTE-V2X radio is half-duplex. A vehicle is then not able to receive a packet while it is transmitting. A *HD* error occurs when a packet is lost because the receiving vehicle is transmitting its own packet in the same sub-frame. The scheduling scheme has an impact on *HD* errors since this

type of error depends on the probability that two vehicles transmit using resources in the same sub-frame.

- 2) Errors due to a received signal power below the sensing power threshold ( $SEN$ ). When a packet is received with a signal power below the sensing power threshold  $P_{SEN}$ , it cannot be decoded and hence a  $SEN$  error is produced. This type of error depends on the distance between the transmitter and the receiver, the transmission power, the propagation and  $P_{SEN}$ .  $SEN$  errors exclude  $HD$  errors.
- 3) Errors due to propagation effects ( $PRO$ ). A  $PRO$  error occurs when a packet is received with a signal power higher than  $P_{SEN}$  but the received SNR (Signal to Noise Ratio) is not sufficient to correctly decode the packet. These errors only account for propagation effects and not for interference and collisions. Then,  $PRO$  errors depend on the same parameters as  $SEN$  errors plus on the MCS.  $PRO$  errors exclude  $HD$  and  $SEN$  errors.
- 4) Errors due to packet collisions ( $COL$ ). These errors occur when two vehicles transmit in the same resource (i.e. the same sub-frame and sub-channel) and the associated SINR (Signal to Interference and Noise Ratio) is not sufficient to correctly decode the packet.  $COL$  errors depend on the distance between the transmitter and the receiver, the transmission parameters, the propagation, the traffic density and the scheduling scheme.  $COL$  errors exclude  $HD$ ,  $SEN$  and  $PRO$  errors.

To analytically model the PDR,  $d_{t,r}$  is considered to be the distance between the transmitter ( $v_t$ ) and the receiver ( $v_r$ ). The model assumes that a packet is correctly received when none of the four possible errors occur. Taking into consideration that these errors are mutually exclusive, the PDR can be obtained as:

$$PDR(d_{t,r}) = \left(1 - \delta_{HD}(d_{t,r})\right) \cdot \left(1 - \delta_{SEN}(d_{t,r})\right) \cdot \left(1 - \delta_{PRO}(d_{t,r})\right) \cdot \left(1 - \delta_{COL}(d_{t,r})\right) \quad (8)$$

where  $\delta_{HD}$ ,  $\delta_{SEN}$ ,  $\delta_{PRO}$  and  $\delta_{COL}$  correspond to the probability of not correctly receiving a packet due to  $HD$ ,  $SEN$ ,  $PRO$  and  $COL$  errors, respectively.

The analytical model proposed in this paper is based on the model proposed in [23], which was designed to evaluate the performance of LTE-V2X Mode 4. In this study, we develop new expressions to quantify  $HD$  and  $COL$  errors for the DIRAC scheduling scheme proposed in this paper for LTE-V2X Mode 3. We utilize the expressions for  $SEN$  and  $PRO$  errors from [23] since they are independent of the scheduling.

To derive the analytical model, we consider a multi-lane highway scenario where vehicles are separated by an approximate distance equal to  $1/\alpha$ . The traffic density is then  $\alpha$  vehicles per meter. All vehicles periodically transmit  $\lambda$  pps. Packets are transmitted on a 10 MHz channel with a transmission power  $P_t$ . To derive the model, we assume all packets have the same size ( $B$ ) and are transmitted using the same MCS. Table II lists all the variables related to the design and operation the DIRAC analytical model.

TABLE II. VARIABLES UTILIZED IN THE DIRAC ANALYTICAL MODEL

Variable	Description
$B$	Packet size
$BL(s)$	BLER for an SNR equal to $s$
$d_{t,r}$	Distance between transmitter and receiver
$d_{t,i}$	Distance between transmitter and interferer
$d_{i,r}$	Distance between interferer and receiver
$n_{max}$	Maximum number of multiples of $d_{reuse}$ or interferers
$N_0$	Noise power
$P_t$	Transmission power
$P_r$	Received signal power
$p'_{SIM}(d_{t,i})$	Probability that $v_t$ and $v_i$ transmit using same resource at the same time.
$p_{INT}(d_{t,r}, d_{t,i})$	Probability that the interference produced by $v_i$ on $v_r$ is higher than a threshold that determines if the packet can be correctly received or not if $v_t$ and $v_i$ simultaneously transmit on the same resource
$PL(d_{t,r})$	Pathloss at $d_{t,r}$
$PDR$	Packet Delivery Ratio
$SNR$	Signal to Noise Ratio
$SINR$	Signal to Interference and Noise Ratio
$v_t, v_r, v_i$	Transmitter vehicle, receiver vehicle and interferer vehicle
$\alpha$	Traffic density (veh/km)
$\delta_{HD}(d_{t,r})$	Probability of not correctly receiving a packet due to half-duplex effect
$\delta_{SEN}(d_{t,r})$	Probability of not correctly receiving a packet due to received signal below sensing threshold
$\delta_{PRO}(d_{t,r})$	Probability of not correctly receiving a packet due to propagation effects
$\delta_{COL}(d_{t,r})$	Probability of not correctly receiving a packet due to collision
$\delta'_{COL}$	Probability of not correctly receiving a packet due to collision caused by interferer $v_i$
$\sigma$	Variance of the shadowing ( $SH$ )
$A_{HD}^n$	Triangular function centered at a certain multiple $n$ of $d_{HD}$
$A_{SIM}^n$	Triangular function centered at a certain multiple $n$ of $d_{reuse}$

### 5.1. HD errors

The probability that a receiving vehicle ( $v_r$ ) cannot receive a packet transmitted by a transmitting vehicle ( $v_t$ ) due to the HD effect is equivalent to the probability that these vehicles are allocated in the same sub-frame. This probability depends on the utilized scheduling scheme. In an ideal scenario, two vehicles using the DIRAC scheduling scheme will suffer the HD effect if they are separated by a distance equal to any positive integer multiple of  $d_{HD}$ . This is the case because the DIRAC scheduling scheme allocates the two vehicles different radio resources in the same sub-frame. In this case,  $v_t$  and  $v_r$  will be able to transmit without their packets but they will not be able to receive each other's transmissions due to the HD nature of the radio transceivers. As a result, the probability that  $v_t$  and  $v_r$  experience a  $HD$  error would be equal to 1 whenever their distance is equal to a multiple of the target HD distance. This probability becomes 0 in any other case since the DIRAC scheduling scheme allocates the two vehicles resources in different sub-frames if their distance is not a positive integer multiple of  $d_{HD}$ . This way, the probability of  $HD$  error would be the sum of a series of unit delta functions at multiples of  $d_{HD}$ . However, the mobility of vehicles complicates an ideal allocation of resources and it is difficult to assign resources ensuring always a distance exactly equal to any positive integer multiple of  $d_{HD}$ . The DIRAC scheduling scheme will try to be as close as possible to these ideal distances. To account for this, we propose to use triangle functions around the multiples of  $d_{HD}$  instead of unit delta functions. As a result, the probability that vehicle  $v_r$  cannot

receive a packet transmitted by vehicle  $v_i$  due to the HD effect is expressed as the sum of multiple triangular functions:

$$\delta_{HD}(d_{t,r}) = \sum_{n \in \mathbb{N}} \Lambda_{HD}^n(d_{t,r}) \quad (9)$$

where each triangular function is centered at  $n \cdot d_{HD}$  and is expressed as:

$$\Lambda_{HD}^n(d_{t,r}) = \begin{cases} \frac{d_{t,r} - d_{HD} \cdot (n-1)}{d_{HD}^2} & \text{if } d_{HD} \cdot (n-1) \leq d_{t,r} \leq n \cdot d_{HD} \\ \frac{d_{HD} \cdot (n+1) - d_{t,r}}{d_{HD}^2} & \text{if } n \cdot d_{HD} < d_{t,r} \leq d_{HD} \cdot (n+1) \\ 0 & \text{else} \end{cases} \quad (10)$$

### 5.2. SEN errors

The probability that a packet is not correctly received because its received signal power is below the sensing power threshold ( $P_{SEN}$ ) does not depend on the used scheduling scheme. Therefore, the probability  $\delta_{SEN}$  derived in [23] can also be applied to our proposed scheduling scheme. The derived calculation takes into consideration the pathloss (PL) and the shadowing (SH). The pathloss is typically modeled with a log-distance function, whereas the shadowing is modeled with a log-normal random distribution with a mean equal to zero and a variance equal to  $\sigma$ . This probability can then be calculated as:

$$\delta_{SEN}(d_{t,r}) = \frac{1}{2} \left( 1 - \text{erf} \left( \frac{P_t - PL(d_{t,r}) - P_{SEN}}{\sigma\sqrt{2}} \right) \right) \quad (11)$$

where  $\text{erf}$  corresponds to the well-known error function,  $P_t$  is the transmission power,  $PL(d_{t,r})$  is the pathloss at  $d_{t,r}$  (i.e. distance between the transmitter and the receiver), and  $\sigma$  is the variance of the shadowing. The details of the calculation of this probability can be found in [23].

### 5.3. PRO errors

The probability that a packet cannot be received due to the propagation effects does not depend on the utilized scheduling scheme. Thus, the probability  $\delta_{PRO}$  calculated in [23] for LTE-V2X Mode 4 is also applicable with our proposed scheduling scheme. This probability depends on the PHY layer performance of the receiver. In this case, the PHY layer performance is modeled by means of the link level LUTs (Look-Up Tables) included in [24]. The LUTs present the BLER (Block Error Rate) as a function of the SNR. Each LUT is provided for a certain packet size, MCS, type of scenario (urban or highway), and relative speed between the transmitter and the receiver. In order to model the *PRO* errors, the SNR at a receiver can be computed as a random variable (in dB):

$$SNR(d_{t,r}) = P_r(d_{t,r}) - N_0 = P_t - PL(d_{t,r}) - SH - N_0 \quad (12)$$

where  $N_0$  corresponds to the noise power. It should be noted that the pathloss is constant for a given distance  $d_{t,r}$ , and hence the SNR follows the same distribution as the shadowing but with a different mean equal to  $P_r - PL - N_0$ . The probability of experiencing a *PRO* error can then be calculated as:

$$\delta_{PRO}(d_{t,r}) = \sum_{s=-\infty}^{+\infty} BL(s) \cdot f_{SNR|P_r > P_{SEN}, d_{t,r}}(s) \quad (13)$$

where

$$f_{SNR|P_r > P_{SEN}, d_{t,r}}(s) = \begin{cases} \frac{f_{SNR, d_{t,r}}(s)}{1 - \delta_{SEN}} & \text{if } P_r > P_{SEN} \\ 0 & \text{if } P_r \leq P_{SEN} \end{cases} \quad (14)$$

The term  $BL(s)$  represents the BLER for an SNR equal to  $s$  and is obtained from the LUTs in [24]. Equation (14) corresponds to the PDF of the SNR at a distance  $d_{t,r}$  for those SNR values for which  $P_r > P_{SEN}$ . This term is used to omit those packets with a received signal power lower than  $P_{SEN}$  (they are already accounted for in  $\delta_{SEN}$ ). The first term of equation (14) corresponds to the  $P_r > P_{SEN}$  condition and is normalized by  $1 - \delta_{SEN}$  in order to ensure that the integral between  $-\infty$  and  $+\infty$  of the PDF of the SNR is equal to 1.

### 5.4. COL errors

*COL* errors are produced when an interfering vehicle  $v_i$  uses the same resource (i.e. the same sub-frame and sub-channel) than the transmitting vehicle  $v_r$ , and the associated interference prevents the correct reception of the packet at  $v_r$  due to a not sufficient level of SINR. Thus, the probability of experiencing a *COL* error depends on the probability that the same resource is allocated to two or more vehicles. The scheduling scheme has a strong impact on  $\delta_{COL}$  and a new model for *COL* errors is necessary for our proposed scheduling scheme. The probability  $\delta_{COL}$  can be expressed as:

$$\delta_{COL}(d_{t,r}) = 1 - \prod_i \left( 1 - \delta_{COL}^i(d_{t,r}, d_{t,i}, d_{i,r}) \right) \quad (15)$$

where  $\delta_{COL}^i$  corresponds to the probability of a *COL* error caused by the interferer  $v_i$ . If  $v_r$  and  $v_i$  simultaneously transmit using the same sub-frame and sub-channel,  $v_i$  can cause a *COL* error if the interference is such that the packet is not correctly received. The probability of a *COL* error caused by  $v_i$  can be expressed as:

$$\delta_{COL}^i(d_{t,r}, d_{t,i}, d_{i,r}) = \sum p_{SIM}^i(d_{t,i}) \cdot p_{INT}(d_{t,r}, d_{i,r}) \quad (16)$$

In equation (16), the term  $p_{SIM}^i(d_{t,i})$  corresponds to the probability that  $v_i$  and  $v_i$  transmit utilizing the same resource at the same time. Thus, this probability depends on the scheduling scheme. The term  $p_{INT}(d_{t,r}, d_{i,r})$  corresponds to the probability that the interference produced by  $v_i$  on  $v_r$  is higher than a threshold that determines if the packet can be correctly received or not if  $v_i$  and  $v_i$  simultaneously transmit on the same resource.

#### 5.4.1. Probability that the interference is higher than a threshold

To calculate  $p_{INT}(d_{t,r}, d_{i,r})$ , we consider the negative effect of the interference caused by  $v_i$  on the receiver  $v_r$  as additional noise [23]. The SINR at the receiver  $v_r$  is then be computed (in dB) as:

$$SINR(d_{t,r}, d_{i,r}) = P_r(d_{t,r}) - P_i(d_{i,r}) - N_0 \quad (17)$$

where  $P_i$  corresponds to the signal power received at the receiver  $v_r$  from the interfering vehicle  $v_i$ . Thus, the SINR consists of a random variable which is obtained from the sum of two random variables, i.e.  $P_r$  and  $P_i$ . Then, the PDF of the SINR can be

computed by means of the cross correlation of the PDF of  $P_r$  and  $P_i$ . Then, the probability that  $v_r$  incorrectly receives a packet due to a low SINR can be expressed as:

$$p_{SINR}(d_{t,r}, d_{i,r}) = \sum_{s=-\infty}^{+\infty} BL(s) \cdot f_{SINR|P_r > P_{SEN}, d_{t,r}, d_{i,r}}(s) \quad (18)$$

The probability in (18) contains packets that cannot be received due to propagation errors. These packets have been taken into consideration in  $\delta_{PRO}$ , so the following normalization is needed to only consider packets lost due to collisions:

$$p_{INT}(d_{t,r}, d_{i,r}) = \frac{p_{SINR}(d_{t,r}, d_{i,r}) - \delta_{PRO}(d_{t,r})}{1 - \delta_{PRO}(d_{t,r})} \quad (19)$$

where  $\delta_{PRO}$  corresponds to the value in equation (13). We assume that the interference is equivalent to additional noise. In this case, the same LUTs from [24] that are used in equation (13) are also used in equation (18) to estimate the value of the BLER in  $BL(s)$ .

#### 5.4.2. Probability that $v_t$ and $v_i$ transmit using the same resource at the same time

The probability  $p_{SIM}^i(d_{t,i})$  that  $v_i$  and  $v_t$  transmit using the same resource at the same time depends on the proposed scheduling scheme. In an ideal scenario, our proposed scheduling scheme would assign  $v_t$  and  $v_i$  the same resource as long as the distance between them is equal to a positive integer multiple of  $d_{reuse}$ . Therefore, there would be a potential interferer associated to each multiple of  $d_{reuse}$ . That would make  $p_{SIM}^i(d_{t,i})$  equivalent to the sum of a series of unit delta functions at multiples of  $d_{reuse}$  for each potential interferer in ideal scenarios. However, in realistic scenarios where vehicles move, the same resource would be assigned to vehicles that are separated by a distance close to a multiple  $d_{reuse}$ , but not necessarily equal. Thus, we propose again the use of triangular functions to realistically model this probability. More specifically, the probability  $p_{SIM}^i(d_{t,i})$  that the interfering vehicle and the transmitting vehicle transmit using the same resource is modelled with the following equation:

$$p_{SIM}^i(d_{t,i}) = \sum_{n \in \mathbb{N}} \Lambda_{SIM}^n(d_{t,i}) \quad (20)$$

where each triangle function is centered at  $n \cdot d_{reuse}$ , and is expressed as follows where  $d_{reuse}$  is named  $d_r$  for clarity:

$$\Lambda_{SIM}^n(d_{t,i}) = \begin{cases} \frac{4 \cdot (d_{t,i} - d_r \cdot (n - \frac{1}{2}))}{d_r^2} & \text{if } d_r \cdot (n - \frac{1}{2}) \leq d_{t,i} \leq n \cdot d_r \\ \frac{4 \cdot (d_r \cdot (n + \frac{1}{2}) - d_{t,i})}{d_r^2} & \text{if } n \cdot d_r < d_{t,i} \leq d_r \cdot (n + \frac{1}{2}) \\ 0 & \text{else} \end{cases} \quad (21)$$

The area under each triangle function is equal to 1 in order to reflect the fact that the scheduler will not assign the same resource to more than one vehicle around  $n \cdot d_{reuse}$ . It should be noted that each positive integer multiple of  $d_{reuse}$  represents a potential interferer  $v_i$ . The number of interferers in the scenario is  $n_{max} = \lfloor d_{max}/d_{reuse} \rfloor$  so  $n \in [1, n_{max}]$ . We should note that our

analytical model and simulation study consider all  $n_{max}$  possible interferers that fit in the scenario. However, interferers at large distances from  $v_t$  have a very small (or even negligible) effect on the signal received by  $v_r$ .

Once  $p_{SIM}^i(d_{t,i})$  is calculated for each interferer  $v_i$  using (20) and (21), the probability  $p_{INT}(d_{t,r}, d_{i,r})$  is computed using (19). Using these probabilities, the probability of experiencing a COL error is calculated for each potential interferer  $v_i$  using (16), and  $\delta_{COL}$  is then calculated with equation (15). The PDR is obtained utilizing equation (8) with the errors  $\delta_{HD}$ ,  $\delta_{SEN}$ ,  $\delta_{PRO}$  and  $\delta_{COL}$  computed using equations (9), (11), (13) and (15), respectively.

## 6. EVALUATION

The proposed DIRAC scheduling scheme has been implemented and evaluated using the Veins simulator. Veins integrates the network simulator OMNeT++ and the road traffic simulator SUMO. The DIRAC scheduling scheme has been implemented in OMNeT++ and has been validated against the analytical model also proposed in this paper. This analytical model has been implemented in Matlab and the source code is available in [22]. The performance of the DIRAC scheduling scheme is compared to the state-of-the-art LTE-V2X Mode 3 algorithm proposed in [16] that has also been implemented in Veins. The performance of the DIRAC scheduling scheme has also been compared to the LTE-V2X Mode 4 scheduling scheme defined by 3GPP [19][25] and described in [26].

### 6.1. Scenario and settings

Simulations are conducted in highway and urban scenarios. Both scenarios have been configured following the 3GPP recommendations in [27]. The highway scenario is 5 km long and has 6 lanes (3 lanes per direction). The traffic density is 120 veh/km and the maximum speed is 70 km/h. Statistics are only taken from vehicles located in the 2 km around the center of the scenario to avoid possible boundary effects. The urban scenario models a Manhattan-like grid layout with 9x7 building blocks of size 433 m x 250 m. All streets have 2 lanes in each direction and each lane is 3.5 m wide. Each street has a 3 m sidewalk on each side. Statistics are collected in the streets and intersections around the center of the scenario in order to avoid border effects. Vehicles are randomly dropped in the scenario and follow random routes. Simulations in the urban scenario are performed considering an average vehicle density of approximately 90 veh/km [27]. The vehicles' mobility is modeled using the traffic simulator SUMO in both highway and urban scenarios. Therefore, vehicles accelerate, decelerate, change lanes and even stop at intersections in the urban scenario.

All vehicles transmit with a power equal to 23 dBm using a dedicated 10 MHz channel at 5.9 GHz. We have analyzed the performance with  $\lambda=10$  pps, 20 pps and 50 pps and packets of 190 bytes. Two sub-channelization configurations are considered: 2 or 4 sub-channels per 1 ms sub-frame. The MCS is selected so that each packet is transmitted using a single sub-channel. In this case, up to 2 packets can be accommodated per sub-frame when considering 2 sub-channels per sub-frame. Similarly, up to 4 packets can be accommodated per sub-frame when 4 sub-channels are considered. MCS 7 is used to transmit packets with 2 sub-channels per sub-frame (25 RBs each). MCS

9 is used to transmit the packets when the channel is divided into 4 sub-channels per sub-frame (12 RBs each). The physical layer performance is modeled using the LUTs in [24] that provide the BLER as a function of the SNR. Following the recommendations in [27], the propagation effects are modeled using the WINNER+ B1 propagation model. For the urban scenario, this model implements a log-distance pathloss model that differentiates between LOS (Line of Sight) and NLOS (Non Line of Sight) conditions. The shadowing is modeled using a log-normal distribution with 3 dB standard deviation for LOS and 4 dB for NLOS. The simulator used in this work implements the In-Band Emission (IBE) model defined by the 3GPP in [27]. IBE can hinder the successful reception of a packet due to ongoing transmissions in adjacent sub-channels of the same sub-frame.

In order to inform the eNB, vehicles send periodically their geographical location to the eNB. The reports are sent every 2 s in this evaluation. These reports consume around 0.55% of the bandwidth available with a 10 MHz channel. The DIRAC scheduling scheme has been tested using other shorter reporting periods and no significant impact on the performance has been observed. This is the case because the location errors resulting from the reporting period are relatively small compared to the target reuse and HD distances.

### 6.2. Validation

Fig. 5 compares the PDR achieved with DIRAC when using simulations (solid lines) and the analytical model (dotted lines) in the highway scenario. The curves are obtained for different packet transmission rates (10 pps, 20 pps and 50 pps) and different channel configurations (4 sub-channels and 2 sub-channels). Fig. 5 clearly shows that the PDR curves closely match for all the configurations that account from low to high channel load levels. The minor differences observed are mostly due to the fact that simulations are carried out under realistic mobility conditions and resources are sequentially assigned upon requests from vehicles. On the other side, the analytical model assumes that allocations are performed for all vehicles at once. Differences are slightly more noticeable for those configurations corresponding to higher congestion levels (e.g. with 50 pps). The close match between the simulation and analytical curves validates both the implementation of our proposed scheduling scheme in the simulation platform and the analytical model.

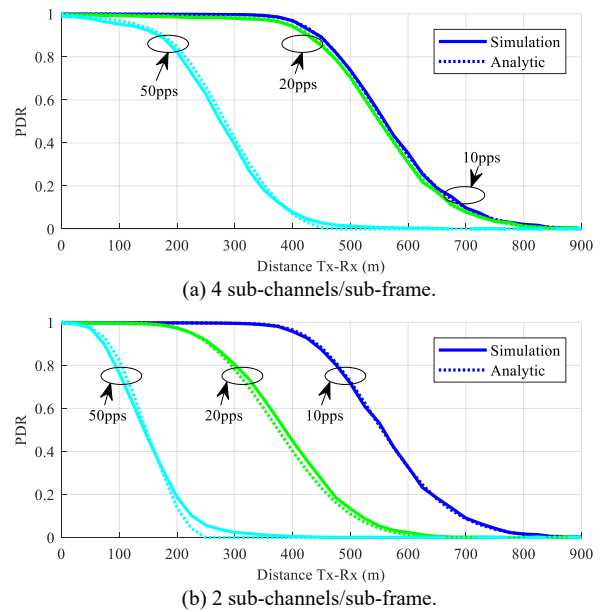


Fig. 5. PDR as a function of the distance between transmitter and receiver for the DIRAC scheduling scheme.

The simulator and the analytical model can differentiate among different types of packet errors, i.e. *HD*, *PRO*, *SEN* and *COL*. Fig. 6 shows the percentage of *HD*, *COL* and *PRO+SEN* errors obtained with the simulator and the analytical model for the scenario with 4 sub-channels per sub-frame (MCS 9) and  $\lambda=50$  pps. Fig. 6 shows that the simulation and analytical results closely match again. The propagation errors (*PRO+SEN*) increase with the distance. This scenario was highly loaded and the average target distances were  $d_{reuse}=667$  m and  $d_{HD}=167$  m. This resulted in that the probability of packet loss due to collision has a peak of more than 80% at around 400 m, and then decreases for farther distances since the propagation errors become more dominant. The probability of *HD* error is nearly constant since this scenario was highly loaded and vehicles using the same sub-frame tend to be close to each other.

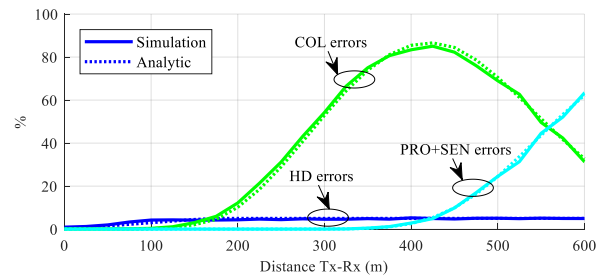


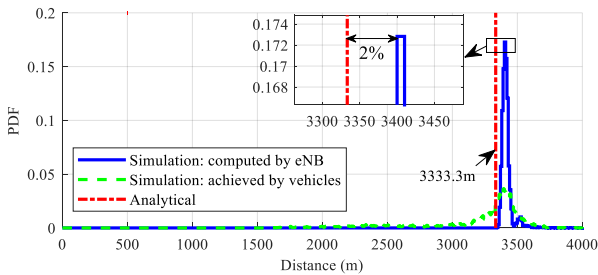
Fig. 6. Percentage of *HD*, *COL*, *PRO* and *SEN* errors as a function of the distance between transmitter and receiver for the DIRAC scheduling scheme. Configuration: 4 sub-channels/sub-frame (MCS 9) and  $\lambda=50$  pps.

Table III shows the analytical values of the target reuse and HD distances for the different scenarios and configurations considered in this study. These values have been obtained with equations (2) and (3) considering 120 veh/km in a 5 km long scenario. The table clearly shows how the target distances are reduced as the resources needed increase (i.e. when the packet rate increase or there is a lower number of sub-channels per sub-frame). Fig. 7 compares the values in Table III with the PDF

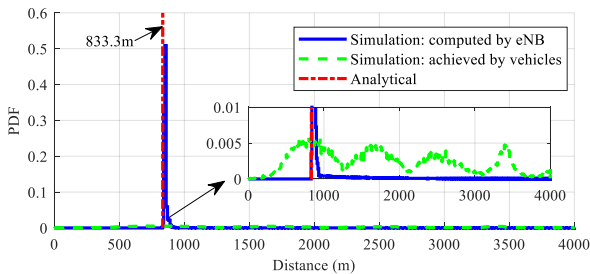
(Probability Density Function) of the target reuse and HD distances computed in the simulations, and the PDF of the reuse and HD distances achieved by the vehicles in the simulations. Fig. 7 has been obtained considering 4 sub-channels per sub-frame (MCS 9) and a packet rate of 10 pps. The figure shows that the eNB computes target values in the simulation close to the analytical ones (e.g. there is around 2% of deviation in the case of the target reuse distance, see Fig. 7a). The small differences result from the fact that the target distances are dynamically computed in the simulations based on the context conditions whereas the analytical values are calculated considering fixed values of  $N_{veh}$  and  $d_{max}$ . Fig. 7 shows that vehicles achieve reuse and HD distances in the simulations around the computed target values. The differences result from the realistic mobility conditions in the simulations. However, Fig. 7 shows that vehicles can operate with reuse and HD distances close to the target values. Fig. 7b shows that vehicles achieve HD distances close to the target value and its multiples. This is due to the fact that the DIRAC scheduling scheme attempts to allocate interfering vehicles separated by a distance close to any multiple of the target distances.

TABLE III. ANALYTICAL TARGET DISTANCES

Number of sub-channels	Packet rate (pps)	$d_{reuse}$ (m)	$d_{HD}$ (m)
4	10	3333.3	833.3
	20	1666.7	416.6
	50	666.7	166.7
2	10	1666.7	833.3
	20	833.3	416.6
	50	333.3	166.7



(a) Reuse distances.



(b) HD distances.

Fig. 7. PDF of the reuse and HD distances achieved in simulations and analytically for the DIRAC scheduling scheme. Configuration: 4 sub-channels/sub-frame (MCS 9) and  $\lambda=10$  pps.

### 6.3. Benchmark scheme

We implement as benchmark scheme the network-controlled resource management algorithm proposed in [16] for LTE-V2X Mode 3. This algorithm has been selected for several reasons.

Authors provide in [16] all the necessary information to implement their proposal, which is not always the case with the proposals presented so far. [16] also demonstrates that the proposal achieves good performance results and is one of the best solutions available so far in the literature. In addition, the proposal in [16] follows an approach that is conceptually opposite to our proposed scheduling scheme, and their comparison would be very valuable to the community to understand the pros and cons of the two approaches. The location-based Mode 3 algorithm proposed in [16] allocates the radio resources based on a pre-defined minimum reuse distance. On the other hand, our solution dynamically adapts the reuse distance to the traffic density and channel load. Moreover, the algorithm in [16] is designed to trigger the resource reselections based on packet errors while DIRAC uses a semi-persistent reservation approach.

The algorithm in [16] exploits the location of vehicles to allocate the resources and is designed to maximize the network’s capacity through the reutilization of resources. The algorithm is designed under the assumption that vehicles periodically transmit beacon messages, and that these messages are intended to be received by all the neighboring vehicles within a certain awareness range  $r_{aw}$ ; this range is an input parameter to the scheduler. The scheduling algorithm is designed to satisfy a minimum reuse range  $r_{reuse}$  that is defined in [16] as the minimum distance at which the same resource can be used by a different transmitter without affecting receivers within the awareness range. The reuse range is calculated following [17] as:

$$r_{reuse} = r_{aw} + \frac{r_{aw}}{\left[ \frac{1}{\gamma_{min}} - \frac{P_{nRB}}{P_{txRB}} \cdot \frac{L_0 \cdot r_{aw}^\beta}{G_r} \right]^\beta} \quad (22)$$

where  $r_{aw}$  is the awareness range,  $\gamma_{min}$  corresponds to the minimum SINR required to decode the message,  $P_{nRB}$  is the noise power over a RB,  $P_{txRB}$  is the transmission power per RB,  $L_0$  is the pathloss at a distance of 1 m,  $\beta$  is the loss exponent, and  $G_r$  corresponds to the antenna gain at the receiver. The pseudo-code of the benchmark algorithm is presented in Algorithm VI. When the eNB receives a request for resources, it first identifies the resources that are utilized by vehicles located within the awareness range of the requesting vehicle (lines 5-16 of Algorithm VI). LTE-V2X operates with HD devices. The eNB discards then all the resources of the sub-frames in which at least one resource is used by a vehicle located within its awareness range ( $r_{aw}$ ) (lines 21-26 of Algorithm VI). Then, the eNB discards the resources that are used by vehicles located outside the awareness range but within the reuse range ( $r_{reuse}$ ) (lines 27-29 of Algorithm VI). Two options are then possible:

(1) If there are more remaining resources than needed for transmitting a packet, the eNB randomly selects the necessary resources among the remaining ones (lines 36-38 of Algorithm VI). The selected resources are allocated to the requesting vehicle on a semi-persistent basis, and reallocations occur as soon as one packet is lost due to poor SINR at a receiver ( $\gamma < \gamma_{min}$ ). In our implementation, we assume that the chipset can measure the RSRP (Reference Signal Received Power) and the

RSSI (Received Signal Strength Indicator) since both metrics are standardized for LTE-V2X Mode 4 and hence available in commercial chipsets. While the RSRP only considers the signal of the TB being decoded, the RSSI also includes all the received interference. The RSRP and RSSI are used to estimate the SINR and recognize if there has been a collision or not. A vehicle then detects a transmission error when it does not successfully decode a TB and the decoding error has been produced due to an interference. Both conditions are necessary to trigger resource reselections.

(2) If the remaining resources are not sufficient to transmit the packet, the eNB cannot allocate resources to the requesting vehicle and the vehicle cannot transmit the packet. The vehicle will request again resources when it generates a new packet. Following [16], the probability that a vehicle cannot transmit a packet increases with the channel load and the awareness range. This can significantly degrade the support of safety-critical V2X services. For a fair comparison with our proposed scheduling scheme, we slightly modify the algorithm in [16] so that a vehicle can also transmit a packet when there are no sufficient remaining free resources. In this case, the vehicle will share resources with another vehicle. To this aim, the eNB dynamically adapts the awareness range (and hence the reuse range). When the eNB receives a request for resources, it tries allocating resources considering a large awareness range. This initial range has been set as of 500 m since larger values would not provide a higher performance due to the propagation effects. If there are not enough remaining resources, the eNB reduces the awareness range in steps of 100 m ( $step=100$ ) until sufficient resources are found (lines 39-42 of Algorithm VI). This is done instead of blocking the transmission of a packet until resources are available again. It should be noted that this modification ensures the use of the highest awareness range (in steps of 100 m) possible that prevents blocking transmissions. Such highest awareness range reduces the interference between vehicles sharing their radio resources.

Algorithm VI. Benchmark scheme from [16]

Inputs:  $N_{SF}$ ,  $N_{SC}$ ,  $N_{veh}$ ,  $r_{aw}$ , pre-computed  $r_{reuse}$ ,  $step$

Output: selected resource  $(j,k)$  for requesting vehicle  $v_{req}$

Execution: every time a vehicle  $v_{req}$  requests resources

---

```

1. Do
2.   For each vehicle  $v_i$  in the scenario with  $1 \leq v_i \leq N_{veh}-1$  do
3.     Get the distance  $d(v_{req}, v_i)$  between  $v_{req}$  and  $v_i$ 
4.   End for
5.   For each sub-frame  $j$  with  $0 \leq j \leq N_{SF}-1$  do
6.     For each sub-channel  $k$  with  $0 \leq k \leq N_{SC}-1$  do
7.       Set  $d_{ref}^{(j,k)}$  equal to  $Inf$ 
8.       For each vehicle  $v_i$  in the scenario with  $1 \leq v_i \leq N_{veh}-1$  do
9.         If  $v_i$  is using resource  $(j,k)$  then
10.          If  $d(v_{req}, v_i) < d_{ref}^{(j,k)}$  then
11.            Set  $d_{ref}^{(j,k)}$  equal to  $d(v_{req}, v_i)$ 
12.          End if
13.        End if
14.      End for
15.    End for
16.  End for
17.  Set  $N_{validResources}$  equal to 0
18.  Create empty list  $validResources$ 
19.  For each sub-frame  $j$  with  $0 \leq j \leq N_{SF}-1$  do
20.    For each sub-channel  $k$  with  $0 \leq k \leq N_{SC}-1$  do
21.      If  $d_{ref}^{(j,k)} \leq r_{aw}$  and  $d_{ref}^{(j,k)} \neq -1$  then
22.        For each sub-channel  $h$  with  $0 \leq h \leq N_{SC}-1$  do
23.          If  $d_{ref}^{(j,h)} \neq -1$  then
24.            Set  $d_{ref}^{(j,h)}$  equal to -1
25.          End if
26.        End for
27.      Else if  $d_{ref}^{(j,k)} \leq r_{reuse}$  and  $d_{ref}^{(j,k)} \neq -1$  then
28.        Set  $d_{ref}^{(j,k)}$  equal to -1
29.      End if
30.      If  $d_{ref}^{(j,k)} \neq -1$  then
31.        Set  $N_{validResources}$  equal to  $N_{validResources}+1$ 
32.        Set  $validResources(N_{validResources})$  equal to resource  $(j,k)$ 
33.      End if
34.    End for
35.  End for
36.  If  $N_{validResources} > 0$  then
37.    Generate random number  $1 \leq i \leq N_{validResources}$ 
38.    Select resource  $(j,k)$  equal to  $validResources(i)$ 
39.  Else
40.    No resource is available,  $r_{aw}$  equal to  $r_{aw} - step$ 
41.  End if
42.  While  $N_{validResources}$  equal to 0 and  $r_{aw} \geq 0$ 

```

---

Fig. 8 depicts the PDR obtained with the original scheduling algorithm proposed in [16] and its modified version. The results are presented for different packet rates (10 pps, 20 pps and 50 pps) and considering 4 sub-channels. For 10 pps, the PDRs are similar since the channel load is low and the original algorithm is able to allocate the required resources without blocking transmissions. However, Fig. 8 shows the effect of blocked transmissions in the original algorithm when the packet rate and channel load increase. In particular, the PDR is highly degraded for 20 pps and 50 pps. This degradation is proportional to the percentage of blocked transmissions. This percentage is equal to 31% and 75% for 20 and 50 pps respectively.

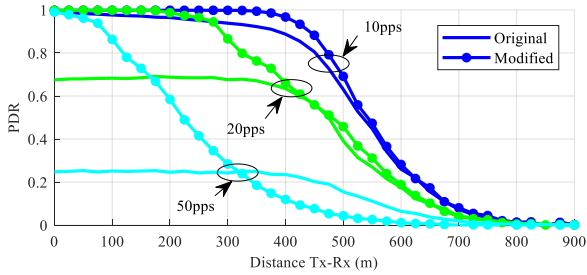
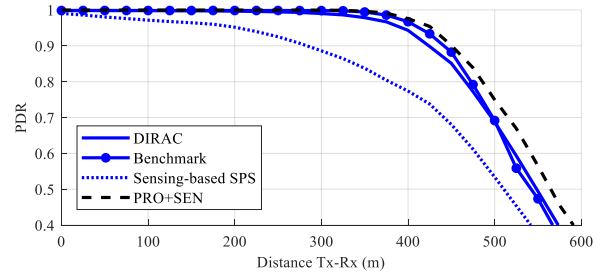


Fig. 8. PDR as a function of the distance between transmitter and receiver for the algorithm from [16]. Configuration: 4 sub-channels/sub-frame (MCS 9).

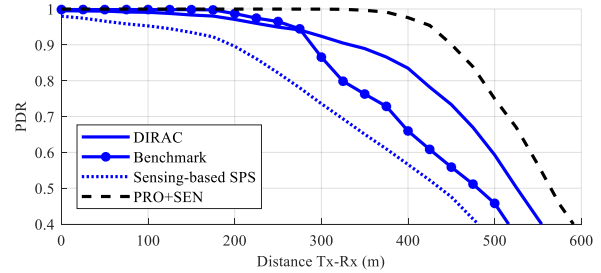
#### 6.4. Comparative analysis

Fig. 9 compares the PDR obtained with the DIRAC scheduling scheme, the modified version of the algorithm proposed in [16], and the LTE-V2X Mode 4 sensing-based SPS algorithm specified by the 3GPP. As an upper bound, Fig. 9 also depicts the PDR that could be obtained without *HD* and *COL* errors, i.e. the PDR that could be achieved when only considering the propagation effects that are independent of the scheduling scheme. Fig. 9 considers the highway scenario with different packet transmission rates, a traffic density of 120 veh/km and 4 sub-channels (MCS 9). Fig. 9a shows that the proposed scheduling scheme, DIRAC, and the benchmark algorithm significantly improve the PDRs for 10 pps compared to LTE-V2X Mode 4. In fact, both algorithms achieve a PDR close to the upper bound. For higher packet rates (Fig. 9b and Fig. 9c), the PDR degrades due to HD errors and packet collisions. It should be noted that such collisions are unavoidable as the load increases and there are limited resources. Fig. 9 shows that the DIRAC scheduling scheme improves the performance over the benchmark algorithm and can better cope with congested scenarios. The figure shows that the gains achieved with DIRAC increase as the load increases due to a more effective allocation of resources thanks to the dynamic computation of the target reuse and HD distances based on the context.

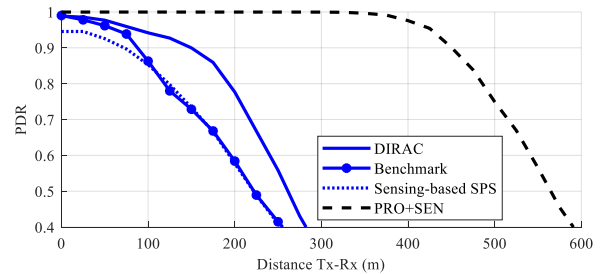
The DIRAC scheduling scheme and the reference scheme have also been evaluated using more congested scenarios i.e. with 2 sub-channels per sub-frame (MCS 7). Fig. 10 compares the PDR obtained with the different schemes for the scenario with 2 sub-channels per sub-frame and a packet transmission rate of 50 pps i.e. the most congested scenario from the considered ones. The obtained results demonstrate that DIRAC still gets a higher performance compared to the benchmark algorithm and LTE-V2X Mode 4. In fact, the DIRAC scheduling scheme stands as the channel load increases thanks to its dynamic allocation of resources that reduces the negative effects of interference and HD transmissions.



(a) 10 pps, 4 sub-channels/sub-frame.



(b) 20 pps, 4 sub-channels/sub-frame.



(c) 50 pps, 4 sub-channels/sub-frame.

Fig. 9. PDR as a function of the distance between transmitter and receiver (highway scenario). Configuration: 4 sub-channels/sub-frame (MCS 9).

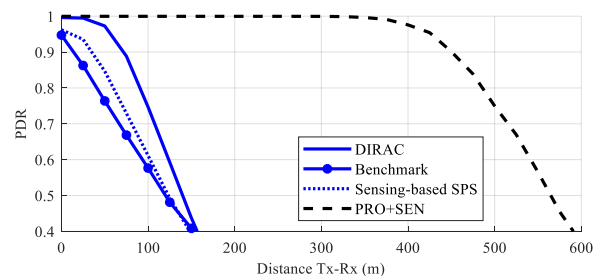


Fig. 10. PDR as a function of the distance between transmitter and receiver (highway scenario). Configuration: 2 sub-channels/sub-frame (MCS 7) and  $\lambda=50$  pps.

Fig. 11 depicts the percentage of packets lost due to collision (*COL*) and propagation errors (*PRO+SEN*) for the highway scenario with 20 pps and 4 sub-channels. *HD* errors are not represented in this figure because they are negligible for this scenario (less than 2%). Since propagation errors do not depend on the scheduling scheme, all schemes experience the same percentage of packets lost due to the propagation effects. Fig. 11 shows that errors due to collisions are predominant up to distances around 450 m since propagation errors are almost null at short distances. For distances higher than 450 m, propagation errors become predominant. Fig. 11 clearly shows that the DIRAC scheduling scheme can significantly reduce packet

collisions compared to the benchmark option and LTE-V2X Mode 4, and maintain packet collisions below 10%. Similar trends were observed in all the scenarios simulated. These results show that the proposed DIRAC scheduling scheme results in an allocation of resources that reduces the negative effects of interference and HD transmissions.

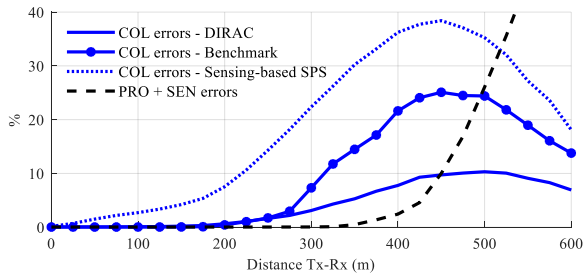


Fig. 11. Percentage of COL, PRO and SEN errors as a function of the distance between transmitter and receiver (highway scenario). Configuration: 4 sub-channels/sub-frame (MCS 9) and  $\lambda=20$  pps.

The previous results show that the proposed DIRAC scheduling scheme improves the performance of LTE-V2X Mode 3 compared to the benchmark scheme. DIRAC also reduces the signal overhead compared to the benchmark scheme. The two schemes generate signaling overhead when vehicles periodically report their location to the eNB and when they request resources to the eNB. Both schemes are configured with the same location reporting period in this study. In this study, these reports consume around 0.55% of the bandwidth available with a 10 MHz channel. However, DIRAC significantly reduces the signaling overhead associated with the request of resources since resources are reallocated less frequently. The benchmark algorithm [16] reallocates resources as soon as there is a transmission error in reception. This generates frequent reallocations due to the mobility of vehicles [16]. Fig. 12 shows how the benchmark algorithm can result in frequent reallocations that increase when the channel load increases. The figure compares the PDF of the number of reallocations per second measured with the benchmark scheme and DIRAC. The figure shows that reallocations (and hence the corresponding signaling overhead) significantly increase with the benchmark scheme as the load increases. In fact, almost every packet requires a reallocation of resources with 20 pps and 50 pps packet transmission rates. This is because as soon as any receiving vehicle detects a transmission error, resources must be reallocated for the transmitting vehicle. DIRAC controls and reduces the reallocations and consequently the signaling overhead through its semi-persistent allocation policy. On average, DIRAC generates one reallocation per second and per vehicle independently of the packet transmissions rate. The resource requests generated by DIRAC consume around 1.09% of the bandwidth available in a 10 MHz channel whereas the benchmark scheme consumes between 6.55% and 54.55% of the bandwidth depending on the packet transmission rate. The results in Fig. 9 and Fig. 10 show that the reduction of the signaling overhead obtained with our scheduling scheme is not achieved at the expense of a degradation of the performance. In fact, DIRAC can improve the performance through an allocation of resources that better combats the negative effects of interference and HD transmissions while reducing the signaling

overhead. As expected, LTE-V2X Mode 4 generates less signaling overhead than the DIRAC scheduling scheme since vehicles autonomously select their resources and do not interact with the eNB. However, our scheme significantly outperforms the LTE-V2X Mode 4 scheduling scheme.

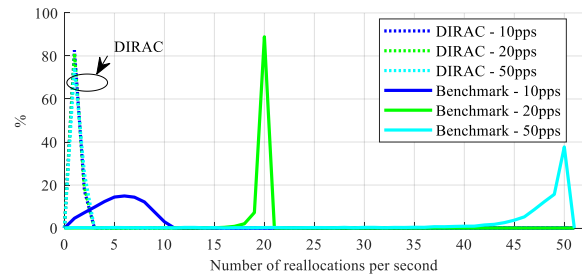
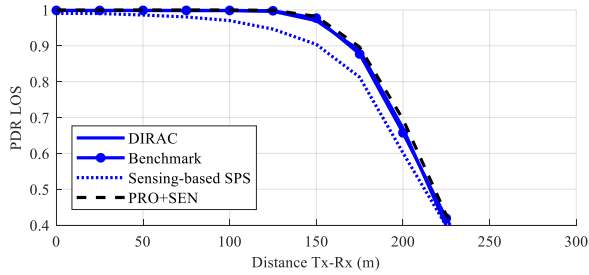


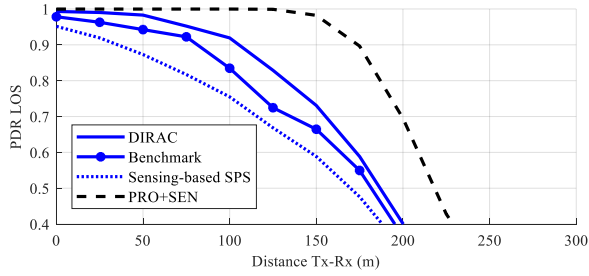
Fig. 12. Number of reallocations per second experienced by the DIRAC scheduling scheme and the modified version of the benchmark algorithm from [16] (highway scenario). Configuration: 4 sub-channels/sub-frame (MCS 9).

Fig. 13 compares the PDR obtained with the DIRAC scheduling scheme, the benchmark scheme and the LTE-V2X Mode 4 scheme in the urban scenario under LOS conditions. Fig. 13 also depicts as an upper bound the PDR that can be achieved when only taking into account the propagation effects that are independent of the scheduling scheme. The figure considers transmission rates of 10 pps (Fig. 13a) and 50 pps (Fig. 13b), and the 4 sub-channels per sub-frame configuration (MCS 9). The figure shows that our DIRAC scheduling scheme and the benchmark scheme achieve a higher PDR than LTE-V2X Mode 4. In particular, both algorithms achieve a similar performance for 10 pps that is close to the upper bound given by the propagation effects. When using a higher packet rate (50 pps), the PDR is degraded due to HD errors and packet collisions that become predominant at lower distances. Nevertheless, under this congested situation, DIRAC clearly outperforms the benchmark scheme, which demonstrates its ability to deal with congested scenarios as it was previously shown for the highway scenario.

Fig. 14 represents the PDR experienced by vehicles that are approaching an intersection under NLOS conditions. These are the most challenging communication conditions in the urban scenario due to the presence of buildings that significantly attenuate the signal level. Fig. 14 shows the PDRs for 10 pps (Fig. 14a) and 50 pps (Fig. 14b) considering the 4 sub-channels per sub-frame configuration (MCS 9). Our DIRAC scheduling scheme and the benchmark scheme achieve a PDR that is close to the upper bound for 10 pps. Both achieve a higher performance than LTE-V2X Mode 4 and DIRAC achieves the highest PDR. The largest improvement obtained with our proposed scheduling scheme is though obtained for 50 pps as shown in Fig. 14b. These results again show that the DIRAC scheduling scheme is able to better cope with higher channel load levels thanks to the dynamic computation of the target distances.

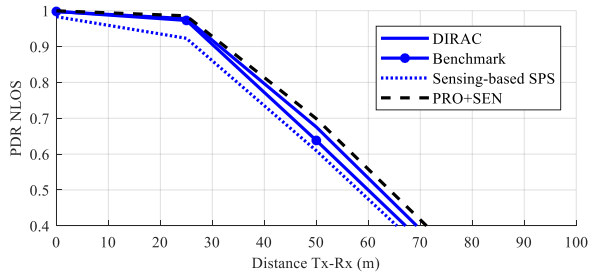


(a) 10 pps, 4 sub-channels/sub-frame.

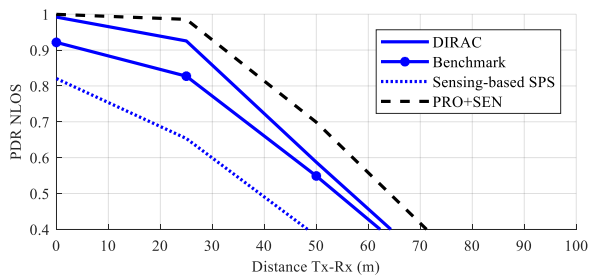


(b) 50 pps, 4 sub-channels/sub-frame.

Fig. 13. PDR as a function of the distance between transmitter and receiver (urban scenario, LOS). Configuration: 4 sub-channels/sub-frame (MCS 9).



(a) 10 pps, 4 sub-channels/sub-frame.



(b) 50 pps, 4 sub-channels/sub-frame.

Fig. 14. PDR as a function of the distance between transmitter and receiver (urban scenario, NLOS). Configuration: 4 sub-channels/sub-frame (MCS 9).

The obtained results demonstrate the high performance achieved by DIRAC scheduling scheme in highway and urban scenarios under realistic mobility conditions. The proposed scheduling scheme outperforms the benchmark algorithm and the LTE-V2X Mode 4 algorithm in both scenarios, especially under high channel load levels. This improvement is achieved thanks to the dynamic adaptation of the target reuse and the target HD distances, which leads to a reduction of the negative effects of packet collisions and HD transmissions.

### 6.5. Computational cost and complexity

The LTE-V2X Mode 3 scheduling schemes analyzed in this work significantly improve the performance of LTE-V2X Mode 4, as illustrated in Section 6.4. This improvement is achieved thanks to the coordination of the resource allocations at the eNB at the cost of an increase in complexity and computational cost.

Algorithm VII presents the pseudo-code of the sensing-based SPS scheme utilized by LTE-V2X Mode 4. The pseudo-code includes the following variables:

- $N_{SF_{sw}}$  is the number of sub-frames in the Sensing Window.
- $SCI$  is an indicator of the received SCIs specifying that a vehicle will utilize the corresponding resource in the Selection Window.
- $threshold$  represents the sensing threshold used in Step 2.
- $T_1$  and  $T_2$  are the limits of the Selection Window.
- $CSR$  represents the Candidate Single-Subframe Resources.
- $L_A$  is the list created by the algorithm that contains the available resources.
- $NE[1, r_{aw}/step]$  represents the number of times the algorithm needs to be repeated until Step 2 is completed.

The pseudo-code distinguishes between the different steps of the sensing-based SPS algorithm. When a vehicle needs to reserve new resources, the vehicle lists first during Step 1 all the  $CSR$  in the Selection Window. In Step 2, the vehicle creates the list  $L_A$  with the available resources and excludes from the  $CSR$  list the resources that meet the following conditions: (1) the vehicle has received in the last  $N_{SF_{sw}}$  sub-frames an  $SCI$  from another vehicle indicating that it will use the corresponding resource in the Selection Window, and (2) the vehicle measures an average RSRP over the resource higher than the  $threshold$ . After Step 2,  $L_A$  must include at least a 20% of the  $CSR$  list. If not, Step 2 is repeated until this target is met. In each iteration, the  $threshold$  is increased by 3 dB. In Step 3, the vehicle creates a list of candidate resources including the resources in  $L_A$  which experienced the lowest average RSSI. The size of this list must be equal to the 20% of the  $CSR$  list from Step 1. The vehicle then randomly selects one of the candidate resources from this list. The details of the operation of this scheme are defined by 3GPP in [19][25] and described in [26].

Algorithm VII. Sensing-based SPS (LTE-V2X Mode 4)  
 Inputs:  $N_{SFsw}=1000$  (Sensing Window),  $N_{SC}$ , sensing results ( $RSRP$ ,  $RSSI$ ,  $SCI$  received, sensing *threshold*),  $T_1$  and  $T_2$  (Selection Window limits)  
 Output: selected resource  $(j,k)$  for requesting vehicle  $v_{req}$   
 Execution: every time a vehicle  $v_{req}$  requests resources

---

**Step 1 and 2**

1. **Do**
2. Create empty list  $CSR$
3. Create empty list  $L_A$
4. Set  $N_{CSR}$  equal to 0
5. Set  $N_A$  equal to 0
6. **For** each sub-frame  $j$  with  $T_1 \leq j \leq T_2$  **do**
7.     **For** each sub-channel  $k$  with  $0 \leq k \leq N_{SC}-1$  **do**
8.         Add resource  $(j,k)$  to  $CSR$
9.         Add resource  $(j,k)$  to  $L_A$
10.         Set  $N_{CSR}$  equal to  $N_{CSR}+1$
11.         Set  $N_A$  equal to  $N_A+1$
12.     **End for**
13. **End for**
14. **For** each sub-frame  $j$  with  $0 \leq j \leq N_{SFsw}-1$  **do**
15.     **For** each sub-channel  $k$  with  $0 \leq k \leq N_{SC}-1$  **do**
16.         **If**  $RSRP(j,k) > \text{threshold}$  and  $SCI$  received in  $(j,k)$  **then**
17.             **If**  $T_1 < j+RRI < T_2$  **then**
18.                 Exclude resource  $(j+RRI,k)$  from  $L_A$
19.                 Set  $N_A$  equal to  $N_A-1$
20.             **End if**
21.         **End if**
22.     **End for**
23. **End for**
24. **If**  $N_A < 0.2 \cdot N_{CSR}$  **then**
25.     Increase *threshold* by 3 dB
26.     Set *repeat* equal to *true*
27. **Else**
28.     Set *repeat* equal to *false*
29. **End if**
30. **While** *repeat* equal to *true*

---

**Step 3**

31. **For** each resource  $L_A(i)$  from list  $L_A$  with  $1 \leq i \leq N_A$  **do**
32.     Set  $RSSI_{LA(i)}$  equal to 0
33.     **For** each  $j$  with  $1 \leq j \leq \lambda$  **do**
34.         Set *aux* equal to  $(1/\lambda) \cdot 1000$
35.         Set  $T$  equal to  $T_{LA(i)} - j \cdot \text{aux}$
36.         Set  $RSSI_{LA(i)}$  equal to  $RSSI_{LA(i)} + RSSI(T)$
37.     **End for**
38.     Set  $RSSI_{LA(i)}$  equal to  $RSSI_{LA(i)}/\lambda$
39. **End for**
40. **Sort** resources  $L_A(i)$  from list  $L_A$  in increasing  $RSSI_{LA(i)}$  associated value
41. Generate random number  $1 \leq n \leq 0.2 \cdot N_{CSR}$
42. Select resource  $L_A(n)$

---

In general, the centralized operation of Mode 3 scheduling schemes increase their complexity compared to the sensing-based SPS scheme defined for Mode 4 that is executed individually by each vehicle. However, this intrinsic higher complexity is assumed by the central scheduler (eNB), which has higher computational capacity. Moreover, this higher complexity results in a significant improvement of sidelink V2X communications as demonstrated in Section 6.4. In any case, the increase of complexity is acceptable for an eNB. The complexity of solving the problem formulated in the DIRAC and benchmark schemes is of order  $O(N_{SF} \cdot N_{SC} \cdot N_{veh})$ . On the other hand, the complexity of solving the problem formulated by the sensing-based SPS scheme is of order  $O(N_{SFsw} \cdot N_{SC})$ . In this case, each vehicle executes the algorithm individually and hence the factor  $N_{veh}$  does not intervene. These complexity values have been obtained from Table IV, Table V and Table VI. These tables present the number of CPU cycles required to execute each line

of the DIRAC, the benchmark and the sensing-based SPS schemes, respectively. The *Repetitions* column corresponds to the number of times each line needs to be executed (many are inside *for* loops). The *Repetitions* column is actually an upper bound since several lines are only executed if a certain condition is satisfied, e.g. lines 9-13 of Step 4 of our DIRAC scheduling scheme. The *Repetitions* column is the one from which the previous complexity orders are obtained. To do so, the complexity order is taken as the highest number of repetitions of a line of the corresponding algorithm, considering all its lines.

The number of CPU cycles is computed considering Intel CPU architectures [28]. For instance, the multiplication of two floating point numbers needs 5 cycles, their division needs 39 cycles, and their addition requires 3 cycles. Using Table IV, Table V and Table VI, we have estimated the upper bound of the total number of CPU cycles required to run each scheme. According to the settings described in Section 6.1, we consider for all the schemes that  $N_{SC}=4$ ,  $N_{veh}=600$  (with a density of 120 veh/km in a scenario with  $d_{max}=5$  km). For DIRAC, we consider  $N^{reuse}_{max}=1$  and  $N^{HD}_{max}=6$  according to the computed target distances, and we assume that Step 1 is not executed. This is equivalent to considering the worst-case scenario because Step 1 is only needed when there are completely free sub-frames, and Step 1 consumes much less CPU than executing the rest of the steps. For the benchmark scheme, we assume that  $r_{aw}=500$  m and  $N=1$  (i.e. we assume the best case in which their algorithm gets to allocate all the resources at the first attempt). Finally, we assume for the sensing-based SPS scheme that  $N_{SFsw}=1000$ ,  $T_1=1$ ,  $T_2=100$ , and  $N_A=0.2 \cdot (T_2-T_1+1) \cdot N_{SC}$ . Assuming a 1GHz ARM Cortex-A9 processor for LTE-V2X Mode 4 and a 3GHz Intel® Core™ i5-8500 processor for the eNB running the LTE-V2X Mode 3 scheduling schemes, Fig. 15 plots the upper bound of the CPU time needed to run each algorithm for a single vehicle request. The figure plots this time as a function of the packet transmission rate  $\lambda$  (i.e. 10 pps, 20 pps and 50 pps). The figure shows that the CPU times decrease as the packet transmission rate increases. This is the case because when the packet transmission rate increases the size of the pool decreases and the number of calculations needed is directly proportional to the number of resources in the pool. Fig. 15 also shows that DIRAC requires a slightly higher CPU time for each individual resource request. However, in the worst case ( $\lambda=10$  pps), the upper bound of the CPU needed to execute DIRAC is around 0.6 ms, which demonstrates the low computational cost of our solution.

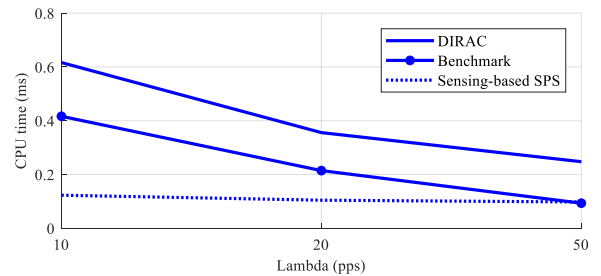


Fig. 15 CPU time needed to run the different schemes per each individual vehicle request as a function of the packet transmission rate. 1GHz processor (LTE-V2X Mode 4) and 3GHz processor (LTE-V2X Mode 3).

Fig. 16 depicts the percentage of CPU time needed to process all the resource requests received per second by the eNB when using the two studied LTE-V2X Mode 3 scheduling schemes. LTE-V2X Mode 4 is not shown in this figure because it is executed individually by each vehicle and there is no need to globally consider all the requests from all the vehicles in the scenario. DIRAC reallocates the resources of a vehicle once per second on average, irrespective of the packet transmission rate. Therefore, DIRAC is executed on average once per second per vehicle and the percentage of CPU time decreases as the packet transmission rate increases, just as the CPU time shown in Fig. 15. The number of reallocations was significantly higher for the benchmark scheme due to its reallocations mechanism, especially for high packet transmission rates (see Fig. 12). As a result, the benchmark algorithm needs to be executed more frequently than our proposed scheduling scheme. This effect is clearly demonstrated in Fig. 16. This figure shows that the overall CPU time needed by the benchmark scheme is significantly higher than the time needed by DIRAC, despite requiring less CPU time per individual vehicle request (Fig. 15). In the worst-case scenario, DIRAC consumes less than 40% of CPU time, but the benchmark scheme requires more than 150% (i.e. more than one processor or CPU thread). These results demonstrate that the performance improvement achieved by DIRAC and demonstrated in Section 6.4 is obtained without increasing the computational cost. In fact, our proposed scheduling scheme, DIRAC, reduces the computational cost by a factor of 3x in the worst-case scenario compared to the benchmark scheme.

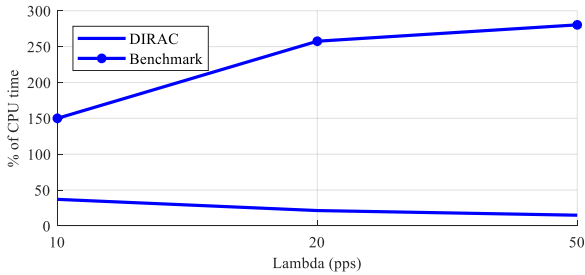


Fig. 16. Percentage of CPU time needed to run the different schemes (per all the requests of all the vehicles in the scenario) as a function of the packet transmission rate. 3GHz processor (LTE-V2X Mode 3).

TABLE IV. COMPUTATIONAL COST OF THE DIRAC SCHEDULING SCHEME

Algorithm line	CPU cycles	Repetitions
<b>Step 1</b>		
1.	1	1
2.	1472	1
3.	1	1
4.	1	1
5.	4	1
6.	1472	1
<b>Step 2</b>		
1.	44	1
2.	44	1
<b>Step 3</b>		
1.	2	$N_{veh}-1$
2.	59	$N_{veh}-1$
3.	1	$N_{veh}-1$
4.	1	$N_{veh}-1$
5.	44	$N_{veh}-1$
6.	44	$N_{veh}-1$
7.	2	$(N_{veh}-1) \cdot N_{reuse}^{max}$
8.	10	$(N_{veh}-1) \cdot N_{reuse}^{max}$
9.	1	$(N_{veh}-1) \cdot N_{reuse}^{max}$
10.	1	$(N_{veh}-1) \cdot N_{reuse}^{max}$
13.	2	$(N_{veh}-1) \cdot N_{HD}^{max}$
14.	10	$(N_{veh}-1) \cdot N_{HD}^{max}$
15.	1	$(N_{veh}-1) \cdot N_{HD}^{max}$
16.	1	$(N_{veh}-1) \cdot N_{HD}^{max}$
<b>Step 4</b>		
1.	1	1
2.	1	1
3.	2	$N_{SF}$
4.	2	$N_{SF} \cdot N_{SC}$
5.	1	$N_{SF} \cdot N_{SC}$
6.	1	$N_{SF} \cdot N_{SC}$
7.	2	$N_{SF} \cdot N_{SC} \cdot (N_{veh}-1)$
8.	1	$N_{SF} \cdot N_{SC} \cdot (N_{veh}-1)$
9.	1	$N_{SF} \cdot N_{SC} \cdot (N_{veh}-1)$
10.	1	$N_{SF} \cdot N_{SC} \cdot (N_{veh}-1)$
12.	1	$N_{SF} \cdot N_{SC} \cdot (N_{veh}-1)$
13.	1	$N_{SF} \cdot N_{SC} \cdot (N_{veh}-1)$
17.	2	$N_{SF} \cdot N_{SC}$
18.	1	$N_{SF} \cdot N_{SC}$
21.	2	$N_{SF} \cdot N_{SC}$
22.	1	$N_{SF} \cdot N_{SC}$
23.	2	$N_{SF} \cdot N_{SC} \cdot N_{SC}$
24.	1	$N_{SF} \cdot N_{SC} \cdot N_{SC}$
25.	1	$N_{SF} \cdot N_{SC} \cdot N_{SC}$
26.	1	$N_{SF} \cdot N_{SC} \cdot N_{SC}$
30.	2	$N_{SF} \cdot N_{SC}$
31.	1	$N_{SF} \cdot N_{SC}$
35.	2	$N_{SF}$
36.	2	$N_{SF} \cdot N_{SC}$
37.	1	$N_{SF} \cdot N_{SC}$
38.	1	$N_{SF} \cdot N_{SC}$
40.	1	$N_{SF} \cdot N_{SC}$
41.	1	$N_{SF} \cdot N_{SC}$
<b>Step 5</b>		
1.	1	1
2.	2	$N_{SF}$
3.	2	$N_{SF} \cdot N_{SC}$
4.	4	$N_{SF} \cdot N_{SC}$
5.	1	$N_{SF} \cdot N_{SC}$
6.	1	$N_{SF} \cdot N_{SC}$
7.	1	$N_{SF} \cdot N_{SC}$

TABLE V. COMPUTATIONAL COST OF THE BENCHMARK

Algorithm line	CPU cycles	Repetitions
2.	2	$N \cdot N_{veh} - 1$
3.	59	$N \cdot N_{veh} - 1$
5.	2	$N \cdot N_{SF}$
6.	2	$N \cdot N_{SF} \cdot N_{SC}$
7.	1	$N \cdot N_{SF} \cdot N_{SC}$
8.	2	$N \cdot N_{SF} \cdot N_{SC} \cdot (N_{veh} - 1)$
9.	1	$N \cdot N_{SF} \cdot N_{SC} \cdot (N_{veh} - 1)$
10.	1	$N \cdot N_{SF} \cdot N_{SC} \cdot (N_{veh} - 1)$
11.	1	$N \cdot N_{SF} \cdot N_{SC} \cdot (N_{veh} - 1)$
17.	1	$N$
18.	1	$N$
19.	2	$N \cdot N_{SF}$
20.	2	$N \cdot N_{SF} \cdot N_{SC}$
21.	2	$N \cdot N_{SF} \cdot N_{SC}$
22.	2	$N \cdot N_{SF} \cdot N_{SC} \cdot N_{SC}$
23.	1	$N \cdot N_{SF} \cdot N_{SC} \cdot N_{SC}$
24.	1	$N \cdot N_{SF} \cdot N_{SC} \cdot N_{SC}$
27.	2	$N \cdot N_{SF} \cdot N_{SC}$
28.	1	$N \cdot N_{SF} \cdot N_{SC}$
30.	1	$N \cdot N_{SF} \cdot N_{SC}$
31.	4	$N \cdot N_{SF} \cdot N_{SC}$
32.	2	$N \cdot N_{SF} \cdot N_{SC}$
36.	1	$N$
37.	1472	$N$
38.	1	$N$
40.	4	$N$
42.	2	$N$

TABLE VI. COMPUTATIONAL COST OF SENSING-BASED SPS

Algorithm line	CPU cycles	Repetitions
<b>Step 1 and 2</b>		
2.	1	1
3.	1	1
4.	1	1
5.	1	1
6.	2	$(T_2 - T_1 + 1)$
7.	2	$(T_2 - T_1 + 1) \cdot N_{SC}$
8.	1	$(T_2 - T_1 + 1) \cdot N_{SC}$
9.	1	$(T_2 - T_1 + 1) \cdot N_{SC}$
10.	4	$(T_2 - T_1 + 1) \cdot N_{SC}$
11.	4	$(T_2 - T_1 + 1) \cdot N_{SC}$
14.	2	$N_{SFsw}$
15.	2	$N_{SFsw} \cdot N_{SC}$
16.	3	$N_{SFsw} \cdot N_{SC}$
17.	1	$N_{SFsw} \cdot N_{SC}$
18.	1	$N_{SFsw} \cdot N_{SC}$
19.	4	$N_{SFsw} \cdot N_{SC}$
24.	1	1
25.	4	1
26.	1	1
28.	1	1
30.	1	1
<b>Step 3</b>		
31.	2	$N_A$
32.	1	$N_A$
33.	2	$N_A \cdot \lambda$
34.	45	$N_A \cdot \lambda$
35.	9	$N_A \cdot \lambda$
36.	4	$N_A \cdot \lambda$
38.	40	$N_A$
40.	3	$N_A \cdot N_A$
41.	1472	1
42.	1	1

## 7. CONCLUSIONS

This paper presents a novel LTE-V2X Mode 3 scheduling scheme, DIRAC, which is designed to homogeneously distribute interference through a dynamic and scalable resource allocation process. To this aim, the DIRAC scheduling scheme exploits the geographical location of the vehicles and adapts the allocation of resources to the context conditions. This reduces packet collisions and the HD effect, and improves the performance compared to LTE-V2X Mode 4 and a benchmark state-of-the-art LTE-V2X Mode 3 scheduling scheme. DIRAC achieves a higher performance while guaranteeing a more stable management of resources that reduces the signaling overhead. The DIRAC scheduling scheme has been validated analytically using a performance model that is also presented in this paper.

The conducted study has revealed interesting open issues that are left for future study. For example, further optimizations would be desirable in scenarios where vehicles have different traffic demands (e.g. different packet transmission rates and/or packet sizes) that may also vary with time and depending on context conditions. A possible approach could be the use of prediction algorithms to anticipate the traffic demand and efficiently schedule the necessary resources.

## ACKNOWLEDGEMENTS

This work was supported by the Generalitat Valenciana and the European Social Fund (ESF) under the research grant ACIF/2018/231, and the support of the Spanish Ministry of Science and Innovation (MCI), the State Research Agency (AEI) and the European Regional Development Fund (FEDER) under project TEC2017-88612-R.

## REFERENCES

- [1] 3GPP TS 36.300, "Evolved Universal Terrestrial Radio Access (E-UTRA) and Evolved Universal Terrestrial Radio Access Network (E-UTRAN); Overall description; Stage 2," Release 16 V16.0.0, Dec. 2019.
- [2] R. Molina-Masegosa and J. Gozalvez, "LTE-V for Sidelink 5G V2X Vehicular Communications: A New 5G Technology for Short-Range Vehicle-to-Everything Communications," *IEEE Vehicular Technology Magazine*, vol.12, no. 4, pp. 30-39, Dec. 2017. DOI: <https://doi.org/10.1109/MVT.2017.2752798>.
- [3] A. Bazzi, G. Cecchini, A. Zanella and B. M. Masini, "Study of the Impact of PHY and MAC Parameters in 3GPP C-V2V Mode 4," *IEEE Access*, vol. 6, pp. 71685-71698, Nov. 2018. DOI: <https://doi.org/10.1109/ACCESS.2018.2883401>.
- [4] R. Molina-Masegosa, J. Gozalvez and M. Sepulcre, "Configuration of the C-V2X Mode 4 Sidelink PC5 Interface for Vehicular Communication," *Proc. 14th International Conference on Mobile Ad-Hoc and Sensor Networks (MSN)*, Shenyang (China), 6-8 Dec. 2018. DOI: <https://doi.org/10.1109/MSN.2018.00014>.
- [5] A. Bazzi, A. Zanella and B. M. Masini, "Optimizing the Resource Allocation of Periodic Messages With Different Sizes in LTE-V2V," *IEEE Access*, vol. 7, pp. 43820-43830, 2019. DOI: <https://doi.org/10.1109/ACCESS.2019.2908248>.
- [6] L. F. Abanto-Leon, A. Koppelaar and S. Heemstra de Groot, "Enhanced C-V2X Mode-4 Subchannel Selection," *Proc. IEEE 88th Vehicular Technology Conference (VTC-Fall)*, Chicago (USA), 27-30 Aug. 2018. DOI: <https://doi.org/10.1109/VTCTFall.2018.8690754>.
- [7] R. Molina-Masegosa, M. Sepulcre and J. Gozalvez, "Geo-Based Scheduling for C-V2X Networks," *IEEE Transactions on Vehicular Technology*, vol. 68, no. 9, pp. 8397-8407, Sept. 2019. DOI: <https://doi.org/10.1109/TVT.2019.2924698>.
- [8] T. Sahin and M. Boban, "Radio Resource Allocation for Reliable Out-of-Coverage V2V Communications," *Proc. IEEE 87th Vehicular*

- Technology Conference (VTC Spring)*, Porto (Portugal), 3-6 June 2018. DOI: <https://doi.org/10.1109/VTCSpring.2018.8417747>.
- [9] 3GPP TS 36.331, "Evolved Universal Terrestrial Radio Access (E-UTRA); Radio Resource Control (RRC); Protocol specification," Release 16 V16.0.0, March 2020.
- [10] L. F. Abanto-Leon, A. Koppelaar and S. Heemstra de Groot, "Parallel and successive resource allocation for V2V communications in overlapping clusters," *Proc. IEEE Vehicular Technology Conference (VNC)*, Torino (Italy), 27-29 Nov. 2017. DOI: <https://doi.org/10.1109/VNC.2017.8275647>.
- [11] L. F. Abanto-Leon, A. Koppelaar and S. Heemstra de Groot, "Subchannel allocation for vehicle-to-vehicle broadcast communications in mode-3," *Proc. IEEE Wireless Communications and Networking Conference (WCNC)*, Barcelona (Spain), 15-18 April 2018. DOI: <https://doi.org/10.1109/WCNC.2018.8377360>.
- [12] L. F. Abanto-Leon, A. Koppelaar and S. Heemstra de Groot, "Network-Assisted Resource Allocation with Quality and Conflict Constraints for V2V Communications," *Proc. IEEE 87th Vehicular Technology Conference (VTC Spring)*, Porto (Portugal), 3-6 June 2018. DOI: <https://doi.org/10.1109/VTCSpring.2018.8417745>.
- [13] J. A. Leon Calvo and R. Mathar, "An Optimal LTE-V2I-Based Cooperative Communication Scheme for Vehicular Networks," *Proc. IEEE 28th International Symposium on Personal, Indoor, and Mobile Radio Communications (PIMRC)*, Montreal (Canada), 8-13 Oct. 2017. DOI: <https://doi.org/10.1109/PIMRC.2017.8292180>.
- [14] R. Fritzsche and A. Festag, "Location-Based Scheduling for Cellular V2V Systems in Highway Scenarios," *Proc. IEEE 87th Vehicular Technology Conference (VTC Spring)*, Porto (Portugal), 3-6 June 2018. DOI: <https://doi.org/10.1109/VTCSpring.2018.8417744>.
- [15] R. Blasco, H. Do, S. Shalmashi, S. Sorrentino and Y. Zang, "3GPP LTE Enhancements for V2V and Comparison to IEEE 802.11p," *Proc. 11th ITS European Congress*, Glasgow (Scotland), 6-9 June 2016.
- [16] G. Cecchini, A. Bazzi, B. M. Masini and A. Zanella, "Localization-Based Resource Selection Schemes for Network-Controlled LTE-V2V," *Proc. 14th International Symposium on Wireless Communication Systems (ISWCS)*, Bologna (Italy), Aug. 2017. DOI: <https://doi.org/10.1109/ISWCS.2017.8108147>.
- [17] A. Bazzi, B. M. Masini and A. Zanella, "How many vehicles in the LTE-V2V awareness range with half or full duplex radios?," *Proc. 15th International Conference on ITS Telecommunications (ITST)*, Warsaw (Poland), May 2017. DOI: <https://doi.org/10.1109/ITST.2017.7972195>.
- [18] G. Cecchini, A. Bazzi, M. Menarini, B. M. Masini and A. Zanella, "Maximum Reuse Distance Scheduling for Cellular-V2X Sidelink Mode 3," *Proc. IEEE Globecom Workshops (GC Wkshps)*, Abu Dhabi (United Arab Emirates), 9-13 Dec. 2018. DOI: <https://doi.org/10.1109/GLOCOMW.2018.8644360>.
- [19] 3GPP TS 36.213, "Evolved Universal Terrestrial Radio Access (E-UTRA); Physical layer procedures," Release 16 V16.1.0, March 2020.
- [20] 3GPP TS 36.211, "Evolved Universal Terrestrial Radio Access (E-UTRA); Physical channels and modulation," Release 16 V16.1.0, March 2020.
- [21] 3GPP TS 36.101, "Evolved Universal Terrestrial Radio Access (E-UTRA); User Equipment (UE) radio transmission and reception," Release 16 V16.5.0, March 2020.
- [22] Open source implementation of the analytical performance model of a LTE-V2X Mode 3 scheduling scheme based on adaptive spatial reuse of radio resources: <https://github.com/msepulcre/C-V2X-mode-3>, 2020 (accessed June 2020).
- [23] M. Gonzalez-Martin, M. Sepulcre, R. Molina-Masegosa and J. Gozalvez, "Analytical Models of the Performance of C-V2X Mode 4 Vehicular Communications," *IEEE Transactions on Vehicular Technology*, vol. 68, no. 2, pp. 1155-1166, Feb. 2019. DOI: <https://doi.org/10.1109/TVT.2018.2888704>.
- [24] R1-160284, "DMRS enhancement of V2V," Huawei, HiSilicon, 3GPP TSG RAN WG1 Meeting #84, St Julian's (Malta), Feb. 2016.
- [25] 3GPP TS 36.321, "Evolved Universal Terrestrial Radio Access (E-UTRA); Medium Access Control (MAC) protocol specification," Release 16 V16.0.0, March 2020.
- [26] R. Molina-Masegosa and J. Gozalvez, "System Level Evaluation of LTE-V2V Mode 4 Communications and its Distributed Scheduling," *Proc. IEEE Vehicular Technology Conference (VTC-Spring)*, Sydney (Australia), 4-7 June 2017. DOI: <https://doi.org/10.1109/VTCSpring.2017.8108463>.
- [27] 3GPP TR 36.885, "Study on LTE-based V2X services," Release 14 V14.0.0, July 2016.
- [28] Intel, "Intel® 64 and IA-32 Architectures Optimization Reference Manual", Order Number: 248966-033, June 2016.

**Daniel Sempere-García** received a Telecommunications Engineering Degree in 2015 and a Master's Degree on Telecommunications Engineering in 2017, both from the Universidad Miguel Hernández de Elche (UMH), Spain. He received Best Academic Record awards both in Telecommunications Engineering Degree and the Master's Degree. He joined the UWICORE research laboratory in May 2016, where he worked on the framework of the CIVIC Project while he was developing his final Master's Degree project, based on short-term traffic forecast by applying Machine Learning techniques and using Floating Car Data from connected vehicles. He is currently conducting his research working on 5G wireless vehicular networks.

**Miguel Sepulcre** received a Telecommunications Engineering degree in 2004 and a Ph.D. in Communications Technologies in 2010, both from Universidad Miguel Hernández de Elche (UMH), Spain. He was awarded by the COIT with the prize to the best Ph.D. thesis. He has been visiting researcher at ESA (The Netherlands), at KIT (Germany), and at Toyota InfoTechnology Center (Japan). He serves as Associate Editor for IEEE Vehicular Technology Magazine and IEEE Communications Letters. He was TPC Co-Chair of IEEE VTC2018-Fall, IEEE/IFIP WONS 2018 and IEEE VNC 2016. He is Associate Professor at UMH, and member of UWICORE research lab working in wireless vehicular networks and industrial wireless networks.

**Javier Gozalvez** received an electronics engineering degree from the Engineering School ENSEIRB (Bordeaux, France), and a PhD in mobile communications from the University of Strathclyde, Glasgow, U.K. Since October 2002, he is with the Universidad Miguel Hernández de Elche (UMH), Spain, where he is currently Full Professor and Director of the UWICORE laboratory. He is the Editor in Chief of the IEEE Vehicular Technology Magazine, and an elected member to the Board of Governors of the IEEE Vehicular Technology Society (IEEE VTS). He was the 2016-2017 President of the IEEE VTS. He was an IEEE Distinguished Speaker and IEEE Distinguished Lecturer for the IEEE VTS.